Available online at www.sciencedirect.com
SCIENCE DIRECT®
Journal of Organometallic Chemistry 690 (2005) 2701–2720
Journal of Organometallic Chemistry
www.elsevier.com/locate/jorganchem

Review

Metallaborane reaction chemistry. Part 12. Some interactions of acetylenes and isocyanides with selected metallaboranes ☆

Jonathan Bould, Mark Bown, Richard J. Coldicott, Evert J. Ditzel, Norman N. Greenwood, Ian Macpherson, Peter MacKinnon, Mark Thornton-Pett, John D. Kennedy *

The School of Chemistry of the University of Leeds, Leeds LS2 9JT, UK

Received 10 December 2004; accepted 10 February 2005
Available online 14 April 2005

Abstract

Compared to the chemistry associated with the basic syntheses and structures of the metallaboranes, their reaction chemistry is relatively uninvestigated. To illustrate the potential variety of such reaction chemistry, a linked overview of some previously reported and previously unreported reactions of the *nido*-6-metalladecaboranes $[(PPh_3)_2HIrB_9H_{13}]$, $[(PPh_3)(Ph_2PC_6H_4)HIrB_9H_{12}]$, $[(\eta^6\text{-}C_6Me_6)RuB_9H_{13}]$, $[(\eta^6\text{-}MeC_6H_4{}^{iso}Pr)RuB_9H_{13}]$ and $[(\eta^5\text{-}C_5Me_5)RhB_9H_{13}]$ with acetylenes and isocyanides is presented, together with some related chemistry derived from the *arachno*-type 4-metallanonaboranes $[(PMe_2Ph)_2PtB_8H_{12}]$ and $[(PMe_3)_2(CO)\text{-}HIrB_8H_{12}]$. Reductions, oligomerisations, and reductive oligomerisations of the unsaturated species are observed, as well as complete or partial incorporation of carbon and nitrogen hetero atoms into the metallaborane clusters.[1]

Keywords: Borane cluster; Metallaboranes; Cluster Aufbau; Cluster expansion; Cluster dismantling; Platinum, ruthenium, iridium and rhodium complexes of boranes and heteroboranes; X-ray crystal and molecular structures; Metallaborane reaction chemistry; Platinaboranes; Iridaboranes; Ruthenaboranes; Rhodaboranes

Contents

☆ This article was freely submitted for publication without royalty. By acceptance of this paper, the publisher and/or recipient acknowledges the right of the authors to retain non-exclusive, royalty-free license in and to any copyright covering this paper, along with the right to reproduce all or part of the copyrighted paper.

* Corresponding author. Tel.: +44 113 343 6414; fax: +44 113 343 6401.
E-mail address: johnk@chem.leeds.ac.uk (J.D. Kennedy).

[1] This paper is an annotated and expanded exposition of an oral presentation at the Third Pan-European Meeting of Boron Chemists, EUROBORON-3, Pruhonice, The Czech Republic, September 2004, of which the proceedings constitute this volume of *Journal of Organometallic Chemistry*.

0022-328X/$ - see front matter © 2005 Elsevier B.V. All rights reserved.
doi:10.1016/j.jorganchem.2005.02.028

1. Introduction

When boron centres in the classical binary boron hydrides are architecturally replaced by metal centres, then metallaboranes result [1–5]. These metallaboranes often conform to the classical *closo-nido-arachno-hypho*, etc. Williams/Wade [6–9] cluster-structure/electron-counting paradigm.

One focus of interest has derived from the findings that experimentally derived metallaboranes are often more stable than their binary boron hydride models, and that this stability can result in metallaborane analogues of those binary boranes of the Williams/Wade paradigm that are themselves not particularly stable, or, sometimes, not isolatable. These are appropriately illustrated by the previously unreported species [4-(η^6-C_6Me_6)-*nido*-4-RuB_5H_9] [compound **1**, Fig. 1 (upper)], a *nido*-B_6H_{10} analogue that may be isolated from the mixture of products from the reaction between [(η^6-C_6Me_6)$RuCl_2$]$_2$ and the [*arachno*-B_6H_{11}]$^-$

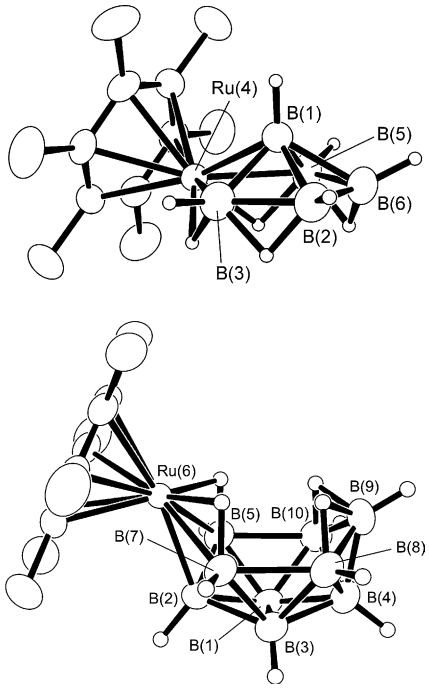

Fig. 1. Crystallographically determined molecular structures of metallaborane analogues of known binary boranes: (top) the *nido*-B_6H_{10} analogue [4-(η^6-C_6Me_6)-*nido*-4-RuB_5H_9] **1** (CCDC 255652); and (bottom) the *nido*-$B_{10}H_{14}$ analogue [6-(η^6-C_6Me_6)-*nido*-6-RuB_9H_{13}] **2a** (CCDC 255653). For a schematic line-drawing of the skeletal structure of **2a**, see Fig. 12. Selected interatomic dimensions (Å) are as follows. For **1**: from Ru(4) to B(1) 2.221(4) to B(3) 2.209(5), to B(5) 2.197(5) to H(3,4) 1.62 (4), to H(4,5) 1.67 (4) and to the six carbon atoms 2.224(4)–2.250(3). For **2a** [Note that there is crystallographic mirror-plane through Ru(6)B(9)B(2)B(4).]: from Ru(6) to C(1) 2.253 (2), to C(2) 2.231(2), to C(3) 2.208 (2), to B(2) 2.218(4), to B(5) 2.233(3) and to H(5,6) 1.70(3); B(10)–B(5) is 2.029 (4) and B(10)–B(9) is 1.777(5).

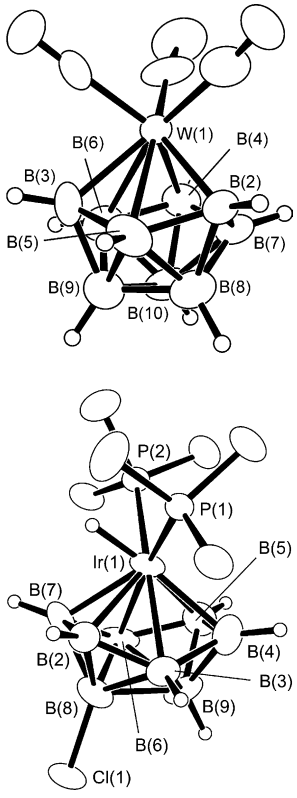

Fig. 2. Crystallographically determined molecular structures of (top) the ten-vertex *isocloso*-structured [1,1,1-$(CO)_3$-*isocloso*-1-WB_9H_9]$^{2-}$ anion **3** as measured in its [NMe_4]$^+$ salt **3a** (CCDC 255654), and (bottom) the nine-vertex *isocloso*-structured neutral species [1,1,1-$(PMe_3)_2$H-*isocloso*-1-IrB_8H_7-8-Cl] **4** (CCDC 255860). Selected interatomic distances (Å) are as follows. For **3**: from W(1) to B(2) 2.234(15), to B(3) 2.260(14), to B(4) 2.227(17), to B(5) 2.520(14), to B(6) 2.507(16) and to B(7) 2.494(17); to C(1) 1.957(12), to C(2)1.955(15) and to C(3) 2.026(16); the corresponding carbonyl C–O distances are 1.181(13), 1.161(16) and 1.132(16), respectively. For **4**: from Ir(1) to P(1) 2.330(2), to P(2) 2.3244(19), to H(1) 1.52(7), to B(2) 2.188(11), to B(3) 2.310(10), to B(4) 2.179(14), to B(5) 2.175(13), to B(6) 2.302(9) and to B(7) 2.210(10); B(8)–Cl(1) is 1.809(11). The angle P(1)–Ir(1)–P(2) is 99.73(8)° and the angle between the vector Ir(1)–H(1) and the plane defined by P(1)Ir(1)P(2) is 65.6(19)°.

anion [10], and also by [6-(η^6-C_6Me_6)-*nido*-6-RuB_9H_{13}] [compound **2a**, Fig. 1 (lower)], a *nido*-$B_{10}H_{14}$ analogue that may be isolated from the mixture of products from the reaction between [(η^6-C_6Me_6)$RuCl_2$]$_2$ and the [*arachno*-B_9H_{14}]$^-$ anion. The isolation of **2a** is previously reported in this Journal [11], but its structure as determined by single-crystal X-ray diffraction analysis is previously unreported. A further example in this category is [2-(η^6-C_6Me_6)-*n*-*arachno*-2-RuB_8H_{14}], an air-stable analogue of the unstable *n*-*arachno* nine-vertex binary borane *n*-B_9H_{15}, isolatable from the products of the reactions of [(η^6-C_6Me_6)$RuCl_2$]$_2$ either with the [*nido*-B_6H_9]$^-$ anion or with the [*arachno*-B_6H_{11}]$^-$ anion [10,12].

A second focus of interest is the ability of transition-element centres in particular to deviate from the bonding patterns that boron centres exhibit. This deviation yields structures that deviate from the classical Williamsian geometrical cluster patterns, as, for example, in the so-called *isocloso*, *isonido* and *isoarachno* cluster geometries [13–15]. Examples of these include the ten-vertex *isocloso*-structured [1,1,1-$(CO)_3$-*isocloso*-1-WB_9H_9]$^{2-}$ anion of C_{3v} symmetry [species **3**, Fig. 2 (upper)] [16], and the nine-vertex *isocloso*-structured neutral species [1,1,1-$(PMe_3)_2$H-*isocloso*-1-IrB_8H_7-8-Cl] [compound **4**, Fig. 2 (lower)] [17]. Of these two species, the tungsten anion **3**, not previously described in detail [18], is formed as the principal reaction product from the reaction of [$W(CO)_3(MeCN)_3$] either with the [*nido*-B_9H_{14}]$^-$ anion or with the [*arachno*-B_9H_{14}]$^-$ anion in the absence of air, and is isolatable as a variety of salts. By contrast, in the presence of air the principal product is the eight-vertex [$(CO)_4WB_7H_{12}$]$^-$ anion of more conventional, albeit rare, *arachno*-type eight-vertex geometry, and of unusual fluxionality [19]. The iridium compound **4** is previously reported as the product from the thermolysis of its *arachno* precursor [4,4,4,4-$(CO)(PMe_3)_2$-H-*arachno*-IrB_8H_{11}-1-Cl] [17]; here we are able to communicate an improved molecular structure obtained by the analysis of a new set of data from a single-crystal X-ray diffraction experiment.

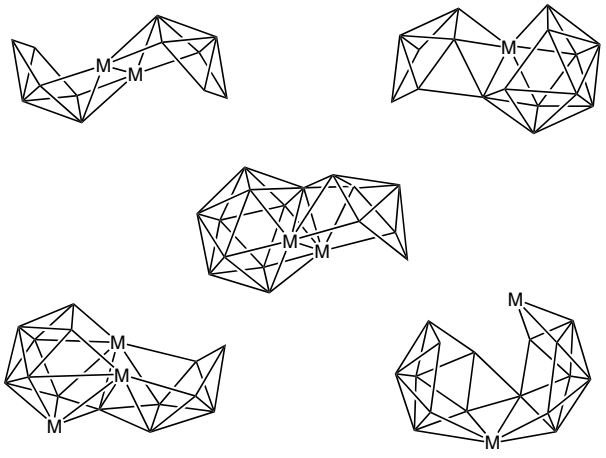

Fig. 3. Schematic representation of the skeletal configurations of (left to right, top to bottom) the macropolyhedral species [$(PMe_2Ph)_2Pt_2B_{12}H_{18}$], [$(PMe_2Ph)PtB_{16}H_{18}(PMe_2Ph)$], [$(PMe_2Ph)_2Pt_2B_{16}H_{15}(C_6H_4Me)$-$(PMe_2Ph)$], [$(PMe_2Ph)_4Pt_3B_{14}H_{16}$] and [$(PMe_2Ph)_3Pt_2B_{16}H_{20}(PMe_2$-Ph)] obtained from thermolysis of [$(PMe_2Ph)_2PtB_8H_{12}$] [23–26].

A third focus of interest is that metal centres can also engender fused multi-cluster assemblies of complex 'macropolyhedral' architectures, which are of increasingly high structural interest [20–23]. For example, mild thermolysis, in toluene or benzene solution, of the *arachno*-structured nine-vertex platinaborane [4,4-$(PMe_2Ph)_2$-*arachno*-4-PtB_8H_{12}] yields a variety of macropolyhedral species, [$(PMe_2Ph)_2Pt_2B_{12}H_{18}$], [$(PMe_2Ph)PtB_{16}H_{18}$-$(PMe_2Ph)$], [$(PMe_2Ph)_2Pt_2B_{16}H_{15}(C_6H_4Me)(PMe_2Ph)$], [$(PMe_2Ph)_4Pt_3B_{14}H_{16}$] and [$(PMe_2Ph)_3Pt_2B_{16}H_{20}(PMe_2$-Ph)], with cluster configurations as illustrated schematically in Fig. 3 [23–26].

These three facets of metallaborane behaviour have dictated that much of the emphasis of metallaborane chemistry has been concerned with their synthesis, either directed or serendipitous, and with their structural characterisation. This synthetic and structural science may be described as the 'first-order chemistry' of the metallaboranes.

The electronic redox flexibility of borane clusters, as manifested, for example, in the two-electron differences in the *closo-nido-arachno-hypho* sequences, allied with the redox flexibility of transition-element centres, implies a very rich metallaborane reaction chemistry based on the reactions of metallaboranes, rather than on their synthesis and structure [27,28]. However, the reaction chemistry of the metallaboranes – which may be described as their 'second-order chemistry' – is relatively neglected. This survey is intended to emphasise and illuminate the vast potential for new science offered by this 'second-order' metallaborane chemistry.

One aspect of high potential interest and potential utility concerns reactions with small multiply bonded organic species. In this paper we therefore present a discursive overview, principally of work carried out in the Leeds laboratories, involving selected reactions of acetylenes and isocyanides with some ten-vertex *nido*-monometallaboranes of general formulation {MB_9H_{13}}, and with some nine-vertex *arachno*-type metallaboranes of general formulation {MB_8H_{12}}, where M represents a transition-element centre. The account is augmented with some closely related cognate chemistry, and is also augmented by some relevant previously unreported crystallographic results.

2. Discussion and results

Reactions to be expected with unsaturated molecules such as isocyanides and acetylenes include additions and oligomerisations and, if catalytic, polymerisations. In

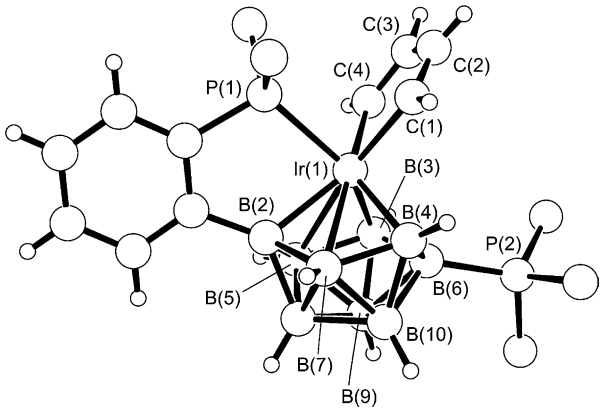

Fig. 4. Crystallographically determined molecular structure of the *isocloso*-clustered species [μ-(Ph_2P-*ortho*-C_6H_4)$C_4H_4IrB_9H_8(PPh_3)$] **6** [34]. For a schematic line-drawing of the skeletal structure, see **II**. Selected interatomic dimensions are as follows. Distances (Å) from Ir(1) are: to P(1) 2.368(4), to B(2) 2.158(9), to B(3) 2.175(10), to B(4) 2.164(9), to B(5) 2.481(9), to B(6) 2.412(9), to B(7) 2.465(10), to C(1) 2.112(8) and to C(4) 2.104(9). Distances within the {C_4Ir} ring are: C(1)–C(2) 1.344(11), C(2)–C(3) 1.453(11) and C(3)–C(4) 1.331(11). Angles about iridium (°) are C(1)–Ir(1)–C(4) 76.6(4), C(1)–Ir(1)–P(1) 86.2(3) and C(4)–Ir(1)–P(1) 80.4(3).

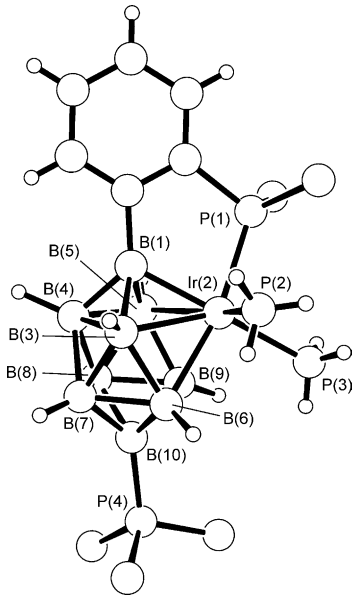

Fig. 5. Crystallographically determined molecular structure of [*μ*–(Ph_2P-*ortho*-C_6H_4)$(PH_3)_2IrB_9H_7(PPh_3)$] **7** [34,35]. Selected interatomic distances (Å) are as follows: Ir(2) to P(1) 2.316(3), to P(2) 2.275(4), to P(3) 2.318(4), to B(1) 2.116(8), to B(3) 2.289(9), to B(5) 2.347(7) and to B(6) 2.273(8). Angles about iridium (°) are: P(1)–Ir(2)–P(2) 93.1(2), P(1)–Ir(2)–P(3) 97.0(2) and P(2)–Ir(2)–P(3) 90.1(2).

view of the hydrogen content of the {B_9H_{13}} and {B_8H_{12}} residues of the selected metallaboranes of generalised formulations {MB_9H_{13}} and {MB_8H_{12}}, reductions are also expected. Incorporation of carbon atoms into the metallaborane clusters is also a probability: for example, it is well-known that the parent ten-vertex non-metalla borane *nido*-$B_{10}H_{14}$ can be induced to react with acetylenes RCCR′ to produce *closo* twelve-vertex dicarbaboranes $RR'C_2B_{10}H_{10}$ [29], and that isocyanides are used to insert single carbon atoms into borane clusters [30,31]. Analogous insertions with metallaboranes would offer alternative 'converse' routes to metallacarbaboranes, which to date have been predominantly synthesised by the addition of metal centres into pre-formed carbaboranes, rather than by the converse process of addition of carbon centres to pre-formed metallaboranes [32,33].

Of these various potential reaction types, oligomerisation is exhibited in the reaction of HC≡CH itself with the *nido*-6-iridadecaborane [6-(PPh_3)-μ-6^P,5^C-(Ph_2P-*ortho*-C_6H_4)-6-H-*nido*-6-IrB_9H_{12}] (compound **5**, schematic I). In refluxing benzene, a species of formulation [(Ph_2P-*ortho*-C_6H_4)$C_4H_4IrB_9H_8(PPh_3)$] (compound **6**, Fig. 4 and schematic skeletal structure **II**) is formed [34]. Dimerisation of HC≡CH has occurred, with the resulting {C_4H_4} unit bound to the iridium centre, generating a five-membered {IrC_4H_4} iridacyclopentadiene ring. The iridium centre retains the *ortho*-cycloboronated {$Ph_2PC_6H_4$} moiety. The cluster overall has lost six hydrogen atoms (Eq. (1)) and has consequently closed, now being of the *isocloso* configuration as also exemplified by species **3** above [Fig. 2 (upper)].

$$[(PPh_3)(Ph_2PC_6H_4)HIrB_9H_{12}]\ \mathbf{5} + 2HC{\equiv}CH \rightarrow [(Ph_2PC_6H_4)C_4H_4IrB_9H_7(PPh_3)]\ \mathbf{6} + 3H_2 \quad (1)$$

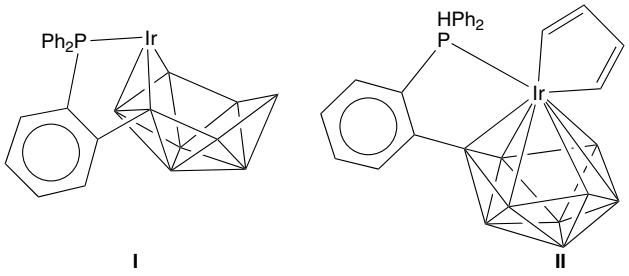

A second product from this reaction, in higher yield, is the species [μ-1^P,2^C-(Ph_2P-*ortho*-C_6H_4)-2,2-$(PH_3)_2$-*closo*-2-IrB_9H_7-10-(PPh_3)] (compound **7**, Fig. 5) [34,35]. There are no {C_2H_2} residues incorporated into this product, but it exhibits the unique phenomenon of a reductive stripping of P-phenyl groups from PPh_3 ligands to give two parent phosphine PH_3 ligands on the metal centre. Again, the *ortho*-cyloboronated {$Ph_2PC_6H_4$} moiety is retained. The compound features a classical *closo* cluster rather than the *isocloso* architecture of compound **5**. The pathway to this unique and intriguing molecule must be complex and no simple stoichiometry can be written down.

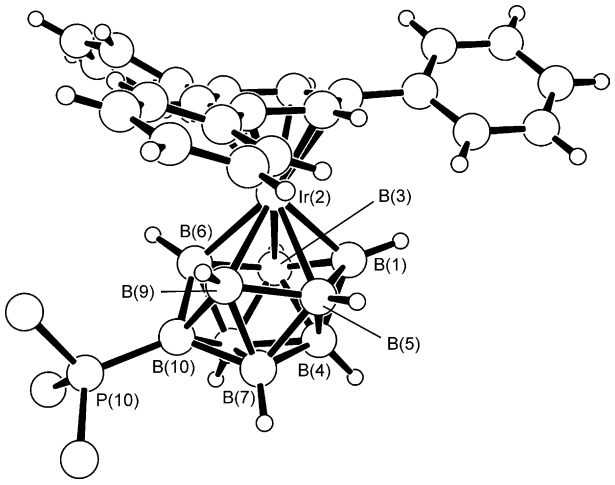

Fig. 6. Crystallographically determined molecular structure of [2-(η^6-$C_6H_3Ph_3$)-*closo*-2-IrB_9H_8-10-(PPh_3)] **9** [36]. Selected interatomic distances (Å) are: from Ir(2) to B(1) 2.078(8), to B(3) 2.257(8), to B(5) 2.247(7), to B(6) 2.223(9) and to B(9) 2.222(8); B(6)–B(9) is 'long' at 2.026(11); other interboron distances are in the range 1.673(11)–1.844(12); B(1)–P(10) is 1.876(9), iridium–carbon distances are in the range 2.248(6)–2.317(6), and intercarbon distances in the hexagonal ring are in the range 1.40(1)–1.44(1).

In contrast to the acetylene dimerisation exhibited in compound **6**, trimerisation can occur when, instead of *ortho*-cyloboronated **5**, the metallaborane substrate is the simpler, non-*ortho*-cyloboronated, analogue of compound **5**, viz. [6,6,6-$(PPh_3)_2$H-*nido*-6-IrB_9H_{13}] (compound **8**), and the acetylene is PhC≡CH. This trimerisation is thence exhibited by the reaction product [2-(η^6-$C_6H_3Ph_3$)-*closo*-2-IrB_9H_8-10-(PPh_3)] (compound **9**, Fig. 6) [36]. In contrast to the dimerisation product **6** in the reaction discussed above, now a PPh_3-substituted conventional *closo* ten-vertex cluster configuration results. However, this now has an aromatic trimerisation product, 1,3,5-$Ph_3C_6H_3$, coordinated η^6 to the iridium centre. A stoichiometry as in Eq. (2) may be written for this process.

$$[(PPh_3)_2HIrB_9H_{13}]\ \mathbf{8} + 3PhCCH \rightarrow [(C_3H_3Ph_3)IrB_9H_8(PPh_3)]\ \mathbf{9} + PPh_3 + 3H_2 \quad (2)$$

In the reactions discussed in the paragraphs above, the acetylene moieties do not become incorporated into the metallaborane clusters. By contrast, in the reaction of acetylene with the *arachno*-structured nine-vertex species [4,4,4,4-$(PMe_3)_2$(CO)H-*arachno*-4-IrB_8H_{12}] (compound **10**), complete cluster incorporation of the two-carbon residue occurs to give [9,9,9-$(PMe_3)_2$(CO)-*nido*-9,8,7-$IrC_2B_8H_{11}$] (compound **11**), of *nido* eleven-vertex constitution (Fig. 7) [37]. This process constitutes a classical 'converse' synthesis of a metalladicarbaborane by the incorporation of the two carbon atoms of an acetylene unit into a metallaborane that initially has no carbon atoms in the cluster. More conventionally, metalladicarbaboranes are synthesised by the addition of metal centres to pre-formed dicarbaboranes [32,33]. The reaction is of straightforward stoichiometry (Eq. (3)).

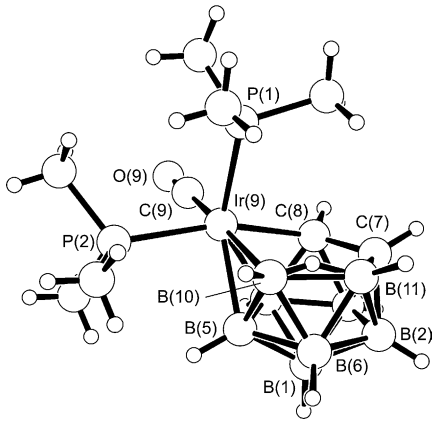

Fig. 7. Crystallographically determined molecular structure of [9,9,9-$(PMe_3)_2$(CO)-*nido*-9,8,7-$IrC_2B_8H_{11}$] **11** [37]. Selected interatomic distances (Å) are: from Ir(9) to P(1) 2.341(2), to P(2) 2.331(2), to C(9) 1.870(6), to C(8) 2.182(7), to B(10) 2.235(6), to B(4) 2.232(7) and to B(5) 2.239(7); C(7)–C(8) is 1.568(9).

$$[(PMe_3)_2(CO)HIrB_8H_{12}]\ \mathbf{10} + C_2H_2 \rightarrow [(PMe_3)_2(CO)IrC_2B_8H_{11}]\ \mathbf{11} + 2H_2 \quad (3)$$

In further contrasting variation, now from the reaction of PhC≡CH with the *arachno*-structured nine-vertex species [4,4-$(PMe_2Ph)_2$-*arachno*-4-PtB_8H_{12}] (compound **12**), cluster incorporation is observed to give a species of formulation [$(PMe_2Ph)_2PtCB_6H_6CPh$] (compound **13**, Fig. 8). This is also a 'converse' metalladicarbabo-

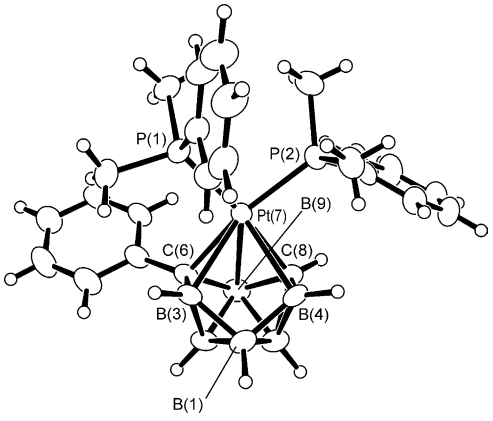

Fig. 8. Crystallographically determined molecular structure of [$(PMe_2Ph)_2PtCB_6H_6CPh$] **13** [38]. For a schematic line-drawing of the skeletal structure, see **IV**. Distances (Å) from Pt(7) are: to P(1) 2.2815(13), to P(2) 2.2770(13), to B(3) 2.442(5), to B(4) 2.449(6), to C(6) 2.1779(5), to C(8) 2.143(5) and to B(9) 2.549(6); selected angles (°) are P(1)Pt(7)P(2) 94.49(5), B(3)Pt(7)B(4) 62.6(2), Pt(7)B(4)B(1) 99.8(3), B(4)B(1)B(3) 97.4(4) and B(1)B(3)Pt(7) 99.8(3). In the quadrilateral open face, Pt(7)–B(1) at 3.201(6) Å and B(3)–B(4) at 2.541(8) Å are both non-bonding, resulting in a skeletal structure that could be considered intermediate between *isonido* and *isocloso*.

rane synthesis [32,33,38], but additional interesting features now occur. Thus, during the course of the formation of this product, two boron atoms are lost to the cluster, and, additionally, the two carbon atoms have become separated to give a 'carbons apart' metalladicarbaborane configuration. An additional interesting factor is that, although compound **13** has a formal *closo* nine-vertex cluster-electron count, it has in fact a very much looser and more open structure than the classical nine-vertex *closo* configuration [14]. Its structure is perhaps best approximated in terms of a *nido*-type $\{H_2CB_6H_6CHPh\}$ unit (schematic **III**, in which unlabelled vertices represent BH(*exo*) units) in which the two CH(*endo*) hydrogen atoms are replaced by bonds to the $\{Pt(PMe_2Ph)_2\}$ moiety (schematic **IV**), resulting in an essentially square planar configuration at the metal centre with much weaker interaction (hatched intracluster connectivity lines in structure **IV**) with the nearest-neighbour boron atoms. Electronic features that contribute to this type of phenomenon in platinaboranes and platinaheteroboranes are adequately discussed elsewhere [15,39,40].

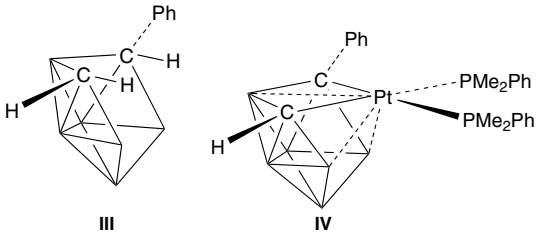

A relevant mechanistic insight into these carbon-atom incorporations that are exhibited by these *nido* ten-vertex metallaborane clusters is afforded by products from the reaction of the *arachno*-type nine-vertex iridaborane [4,4,4,4-$(PMe_3)_2$(CO)H-4-IrB_8H_{12}] (compound **10**) with the 'ene-yne' acetylene CH_2═CMe-C≡CH [41]. Thus, one product of this reaction is the *nido* eleven-vertex cluster species [7-{$C(CH_3)CH_2$}-9,9,9-(CO)$(PMe_3)_2$-*nido*-9,7,8-$IrC_2B_8H_{10}$] [compound **14**, Fig. 9 (upper)], in which cluster-*Aufbau* by complete incorporation of the two-carbon acetylene residue into the *arachno* nine-vertex $\{IrB_8\}$ cluster has occurred to give a *nido* eleven-vertex $\{IrC_2B_8\}$ species, in close analogy to the conversion of compound **10** to compound **11** itemised above (Eq. (3)). This observation further reinforces the concept of 'converse' metalladicarbaborane construction. In this conversion of **10** to **14**, there are strong elements of similarity to the classical reaction of ten-vertex *nido*-$B_{10}H_{14}$ with acetylenes to give twelve-vertex $\{C_2B_{10}\}$ dicarbaboranes [29], as mentioned above.

The second product of the reaction between the nine-vertex iridaborane **10** and CH_2═CMe─C≡CH,

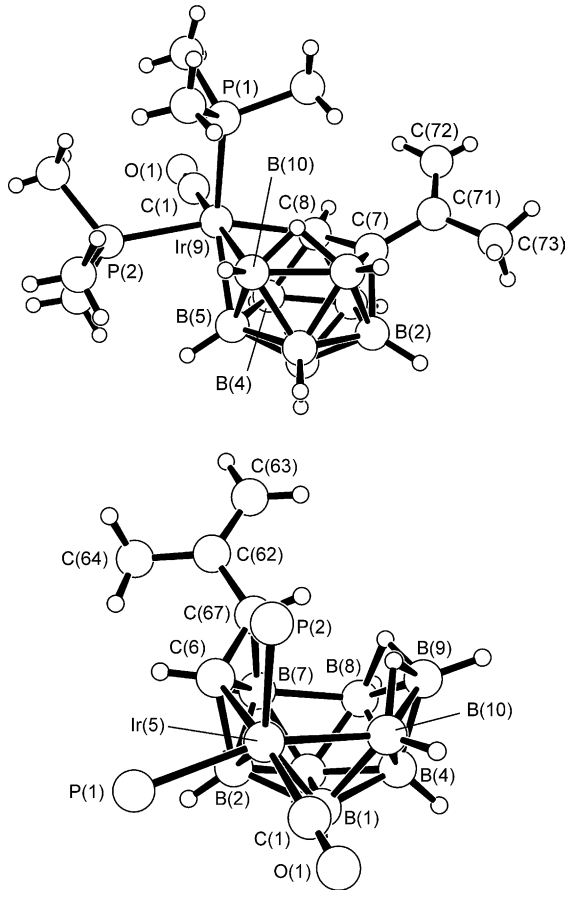

Fig. 9. Crystallographically determined molecular structures of (upper) [(CO)$(PMe_3)_2IrB_8H_{10}C_2${C(Me)═CH_2}] **14** and (lower) [(CO)$(PMe_3)_2IrB_8H_{10}$C(CHC(Me)═CH_2)] **15** from the reaction of CH_2═C(Me)─C≡CH with compound **10** [41]. Compound **14** shows an assimilation of the two carbon atoms of the acetylinic residue to give an eleven-vertex $\{IrC_2B_8\}$ *nido* cluster, whereas **15** shows the incorporation of one carbon atom into the nine-vertex iridaborane cluster. Selected interatomic dimensions (Å) are as follows. For **14**: from Ir(9) to P(1) 2.3456(11), to P(2) 2.3278(11), to B(4) 2.220(5), to B(5) 2.235(5), to C(8) 2.192(4) and to B(10) 2.257(5); C(7)–C(8) is 1.541(6) and olefinic C(71)–C(72) is 1.330(6). For **15**: from Ir(5) to P(1) 2.3710(14), to P(2) 2.345(2), to B(2) 2.219(6), to B(10) 2.254(6) and to C(6) 2.162(5); C(6)–B(7) is 1.826(7), C(6)–C(61) is 1.495(7), B(7)–C(61) is 1.673(8), and olefinic C(62)–C(63) is 1.359(9). The angle C(6)–C(61)–B(7) is 70.1(3)°.

viz., a species of formulation [5,5,5-(CO)$(PMe_3)_2$-μ-6,7-{$CHC(CH_3)CH_2$}-*nido*-5,6-$IrCB_8H_{11}$] [compound **15**, Fig. 9 (lower)] is perhaps of some mechanistic significance [41]. It shows the incorporation of one carbon atom into the nine-vertex iridaborane cluster matrix. It also shows a partial involvement of the second carbon atom with the resulting ten-vertex $\{IrCB_8\}$ system. It is also apparent that an effective reduction of the acetylene residue of the original ene-yne substrate is occurring. A molecule of compound **15** may therefore model a pertinent interesting mechanistic snapshot. Firstly, it freezes the process of incorporation of two carbon atoms of an acetylinic residue at the stage of

the incorporation of one carbon atom, and it also shows the incipient incorporation of the second carbon atom. This may have general generic mechanistic implications for acetylene incorporation into boron-containing cluster species. Secondly, there is an incipient reduction of the acetylenic residue by the utilisation of the hydrogen atoms of the hydrogen-rich open face of the starting iridaborane **10**. The cluster of **15** is thence notionally at a point of decision: (a) whether to incorporate the entire acetylenic residue to form a bigger cluster, or, (b) to reduce, and possibly extrude, the two carbon atoms of the acetylenic residue, in an overall reaction for acetylene reduction. The first of these two consequences may therefore have relevance to generic philosophies for the incorporation of two acetylenic carbon atoms into boron-containing clusters in general, as just mentioned. The second may have potential value in the tailoring of metallaboranes for designed reductions of unsaturated organic species, even though in this present example no reductive extrusion has yet been established, since non-boron-containing residues from this reaction or, for example, from the reaction of iridaborane **5** with HC≡CH to give compounds **6** and **7** mentioned above, have not yet been investigated and elucidated.

Interestingly, and in contrast to the reaction of the $\{PtB_8\}$ platinaborane **10** to give the $\{PtC_2B_6\}$ platinadicarbaborane **11** discussed above, no boron atoms are lost in these iridaborane conversions with acetylenes. This may be a consequence of the greater flexibility of electronic and orbital contribution of the iridium centre compared to that of platinum: in particular, for iridium there is an apparent greater ability readily to move hydridic hydrogen atoms between boron-bound and iridium-bound positions [17,37] (see also below near Eq. (9)).

Isocyanides, RN≡C, also have reactive triply bonded character, with many analogies to acetylenes. In accord with this type of parallel, we have found that, in reactions of *nido*-6-metallaboranes with organyl isocyanides, both hetero-atom incorporation into the metallaborane cluster and also reductive extrusion processes can now be observed, as well as loss of boron atoms. These competing types of behaviour are exemplified by the chemistry described in the following paragraphs.

Thus, the two alternative processes of hetero-atom incorporation and reductive extrusion are exhibited in reactions of organyl isocyanides with the ten-vertex *nido*-6-metalladecaboranes [6-(η^5-C_5Me_5)-*nido*-6-RhB_9H_{13}] (compound **16**), [6-(η^6-C_6Me_6)-*nido*-6-RuB_9H_{13}] (compound **2a**, Fig. 1 above) and [6-(η^6-$MeC_6H_4^{iso}Pr$)-*nido*-6-RuB_9H_{13}] (compound **2b**). Thence, of these, compound **2a** has been shown to react with MeNC [42]: upon gentle heating the ultimate products of the reaction are dimethylamine (Me_2NH) and the *isocloso*-structured ruthenadecaborane [1-(η^6-C_6Me_6)-*isocloso*-RuB_9H_9] (compound **17a**). A simple stoichiometry as in Eq. (4) can be written down for this overall process [41,43].

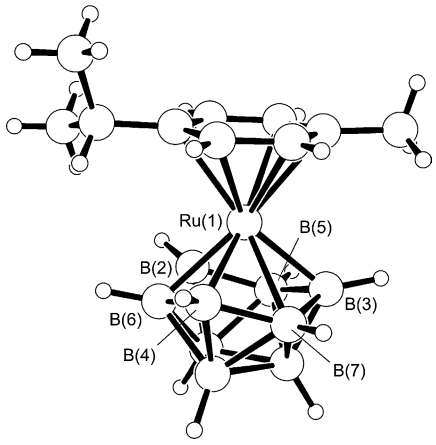

Fig. 10. Crystallographically determined molecular structure of *isocloso*-structured [(η^6-$MeC_6H_4^{iso}Pr$)RuB_9H_9] **17b** [45]. For a schematic line-drawing of the skeletal structure, see Fig. 12. Compare species **3**, Fig. 2. Selected interatomic dimensions are as follows: selected interatomic distances (Å) are: Ru(1) to B(2) 2.143(4), to B(3) 2.146(4), to B(4) 2.137(4), to B(5) 2.315(4), to B(6) 2.299(4), to B(7) 2.311(4) and to C(aryl) 2.290(3)–2.358(3).

$$ArRuB_9H_{13} + MeCN = ArRuB_9H_9 + Me_2NH \quad (4)$$

The methyl isocyanide has undergone a four-hydrogen reduction to give dimethylamine, and the $\{B_9H_{13}\}$ unit of compound **2a** has undergone a corresponding four-hydrogen oxidation to yield the $\{B_9H_9\}$ residue of [1-(η^6-C_6Me_6)-*isocloso*-RuB_9H_9] **17a**. The $\{ArRuB_9H_9\}$ structural type is represented by the *para*-cymene analogue [(η^6-$MeC_6H_4^{iso}Pr$)RuB_9H_9] (compound **17b**, Fig. 10), obtained from a closely related reaction system that starts from [6-(η^6-$MeC_6H_4^{iso}Pr$)-*nido*-6-RuB_9H_{13}] (species **2b**) rather than from the $\{Ru(C_6Me_6)\}$ species **2a** [44]. Compound **17b** has also been isolated from the reaction between [$\{RuCl_2(\eta^6$-$MeC_6H_4^{iso}Pr)\}_2$] and the [*arachno*-B_9H_{14}]$^-$ anion [45].

The four-hydrogen redox process of Eq. (4) must involve several steps, involving an initial association of the isocyanide with the metallaborane unit, a succession of hydrogen-atom transfers, and the ultimate extrusion of the reduced MeNC moiety as Me_2NH. By following the reaction by NMR spectroscopy, and by the isolation of other species from this and closely related reactions, structural types along the reaction coordinate can be identified, and in some cases we have been able unequivocally to characterise these structural models by single-crystal X-ray diffraction analyses. Thus the species [6-(η^5-C_5Me_5)-6-(EtNC)-*arachno*-6-RhB_9H_{11}-9-(EtNC)] (compound **18**, Fig. 11), isolatable as an initial reaction product from the reaction between [6-(η^5-C_5Me_5)-*nido*-6-RhB_9H_{13}] (compound **16**) and ethyl isocyanide, EtNC, demonstrates an initial addition of isocyanide

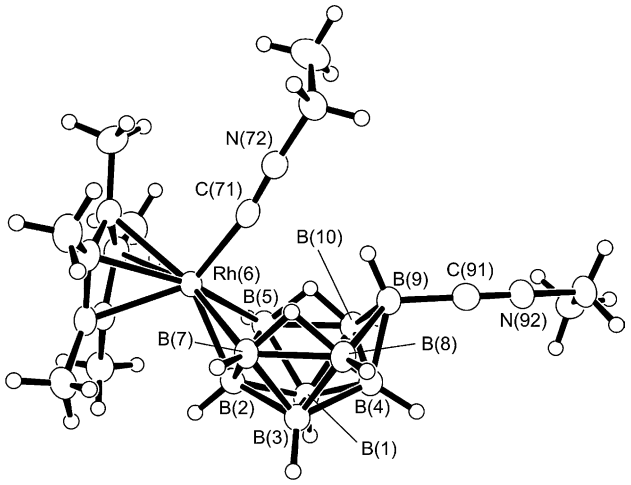

Fig. 11. Crystallographically determined molecular structures of [6-(η^5-C_5Me_5)-6-(EtCN)-*arachno*-6-RhB_9H_{11}-9-(EtCN)] **18** (CCDC 255856). Selected interatomic distances (Å) are: Ru(1) to B(2) 2.182(2), to B(5) 2.256(2), to B(7) 2.269(2), to C(71) 1.929(2) and to C(aryl) 2.234(2)–2.263(2); B(9)–C(91) is 1.552(3), C(91)–N(92) is 1.144(2) and C(71)–N(72) is 1.157(3).

moieties to the *nido* ten-vertex $\{MB_9H_{13}\}$ metallaborane unit, albeit with dihydrogen loss (Eq. (5)).

$$ArRhB_9H_{13} + 2RNC \rightarrow [Ar(RNC)RhB_9H_{11}(NCR)] + H_2 \quad (5)$$

This is another reaction that has a direct parallel with the very well-known reaction of *nido*-$B_{10}H_{14}$ itself with two-electron ligands L to give *arachno* [6,9-L_2–$B_{10}H_{12}$] species [46], and, in accord with this, the molecular structure of **18** (Fig. 11) is clearly seen to be of the *arachno* ten-vertex type, with bridging hydrogen atoms on the open-face B(5)–B(10) and B(7)–B(8) positions, and with the added EtCN units being positioned one-*exo*/one-*endo* in the cluster 6- and 9-positions, as observed, for example, in the initial product [*exo*-6-*endo*-9-(PMe_2Ph)$_2$-*arachno*-$B_{10}H_{12}$] from the reaction of *nido*-$B_{10}H_{14}$ with excess PMe_2Ph [47,48].

It is, however, unlikely that bis(isocyanide) species such as **18** are direct intermediates in the process of Eq. (4), because this last process would require the utilisation of all four bridging hydrogen atoms of compounds **2a** and **2b** for the complete reduction of MeNC to Me_2NH, whereas from Eq. (5) it can be seen that two of these four hydrogen atoms would be lost to the system prior to any such reduction. The monitoring of the reaction system involving MeNC and the {Ru(η^6-C_6Me_6)} compound **2a** by NMR spectroscopy does, however, show an unstable intermediate of formulation $\{(C_6Me_6)RuB_9H_{11}(CH_2NMe)\}$ (species **19**, proposed schematic representation as in Fig. 12), which can be isolated as an orange solid [42]. In this last species **19**

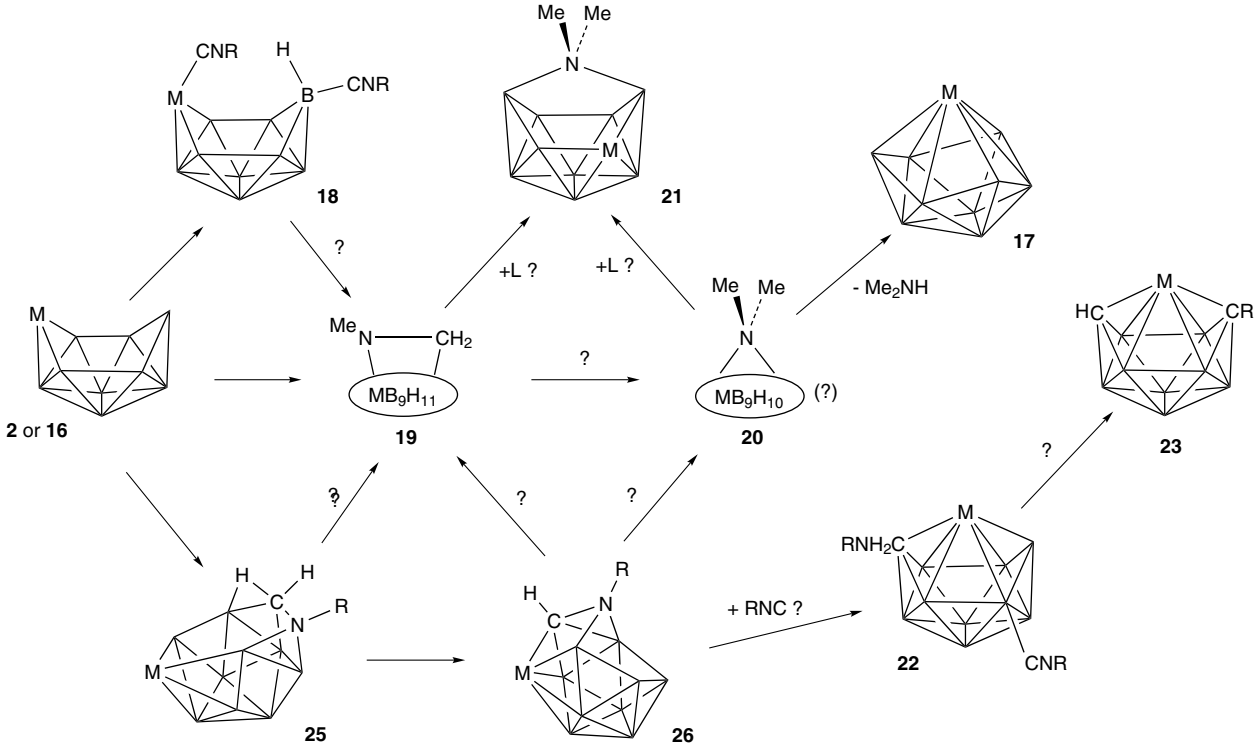

Fig. 12. Schematic skeletal structures of reactants, proposed intermediates, isolated products, and isolated species that possibly represent structural models of proposed intermediates, from reaction systems involving organyl isocyanides RNC with [6-(η^6-C_6Me_6)-*nido*-6-RuB_9H_{13}] **2a**, [6-(η^6-$MeC_6H_4^{iso}Pr$)-*nido*-6-RuB_9H_{13}] **2b** and [6-(η^5-C_5Me_5)-*nido*-6-RhB_9H_{13}] **16**. Crystallographically determined molecular structures of representatives of the structure types indicated by the bold numbers are to be found in the figures as follows: **2** Fig. 1, **17** Fig. 10, **18** Fig. 11, **21** Fig. 13, **22** Fig. 14, **23** Fig. 14, **25** Fig. 15 and **26** Fig. 16. Structures numbered **19** and **20** are proposed intermediates as discussed in the text.

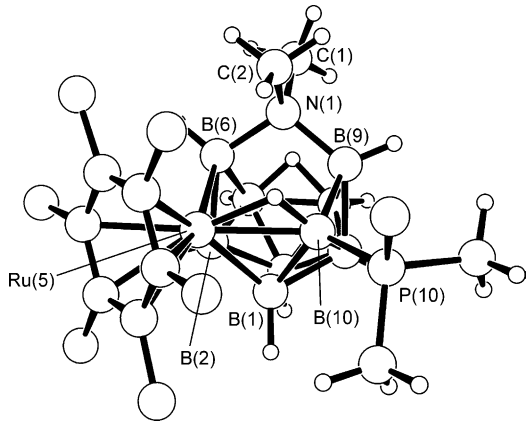

Fig. 13. Crystallographically determined molecular structure of [(η^6-C_6Me_6)RuB_9H_{10}(PMe_2Ph)(NMe_2)] **21** [42]. For a schematic line-drawing of the skeletal structure, see Fig. 12. Selected interatomic distances (Å) are as follows: from Ru(1) to B(1) 2.212(5), to B(2) 2.178(5), to B(6) 2.300(5) and to B(10) 2.319(5), and to C(aryl) (mean) 2.245(4); from N(1) to C(1) 1.532(6), to C(2) 1.506(6), to B(6) 1.625(6) and to B(9) 1.615(6).

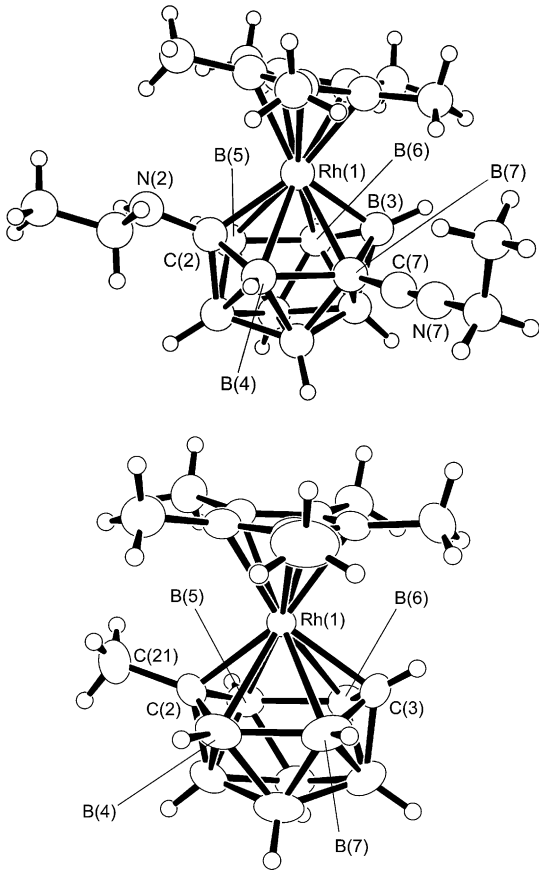

Fig. 14. Crystallographically determined molecular structures of (upper) [1-(η^5-C_5Me_5)-*closo*-1,2-$RhCB_9H_9$-7-(CNEt)-2-(NH_2Et)] **22** and (lower) [1-(η^5-C_5Me_5)-*closo*-1,2,4-$RhC_2B_8H_9$-2-Me] **23** [52]. For a schematic line-drawing of the skeletal structures see Fig. 12. Selected interatomic distances (Å) are as follows. For **22**: from Ru(1) to C(2) 2.164(4), to B(3) 2.121(5), to B(4) 2.461(5), to B(5) 2.384(5), to B(6) 2.354(5), to B(7) 2.362(5), and to C(cyclopentadienyl) 2.177(4)–2.283(4); C(2)–N(2) is 1.416(4) and B(7)–C(7) is 1.533(6). For **23**: from Ru(1) to C(2) 2.115(4), to C(3) 2.089(4), to B(4) 2.366(5), to B(5) 2.376(5), to B(6) 2.396(5), to B(7) 2.374(5), and to C(cyclopentadienyl) 2.185(4)–2.209(4); C(2)–C(21) is 1.520(6).

the {–CH_2–NMe–} unit is linked to the cluster, but this species has so far proved to be unstable under the separatory conditions that we have been able to use, and has consequently so far defied isolation in a pure crystalline state, and thence unequivocal characterisation. However, the NMR evidence strongly suggests a partial, two-hydrogen, reduction of the MeNC moiety. From such a species, an additional two-hydrogen reduction and thence extrusion of the resulting Me_2NH would generate the observed ultimate [(η^6-C_6Me_6)RuB_9H_9] product **17a**. This may imply a penultimate Me_2N-bridged intermediate {(η^6-C_6Me_6)RuB_9H_{10}(NMe_2)} (species **20**), which would require just one hydrogen-atom transfer to complete the stoichiometry of Eq. (4).

In regard to such a proposed intermediate of the form of **20** we have found that the quenching of the reaction at the **19/20** stage by the addition of PMe_2Ph (Fig. 12) results in the formation of the isolatable {NMe_2}-bridged compound of formulation [(C_6Me_6)RuB_9H_{10}-(PMe_2Ph)(NMe_2)] (compound **21**, Fig. 13) [42]. The cluster of **21** is of *arachno* ten-vertex {RuB_9} constitution, and in accord with this, and as with the *arachno* ten-vertex compound **18** above (Fig. 11), it exhibits diagnostic open-face bridging hydrogen atoms at the cluster (5,10) and (7,8) positions. Interestingly, the metal atom is now in the 5-position in this quenched-out species, rather than in the 6-position. The nitrogen-atom of the {NMe_2} residue is effectively a bifurcating bidentate centre that coordinates *endo* to each of the B(6) and B(9) positions, and thereby has a contrasting but electronically equivalent configuration to the {*exo–exo*} coordination most typically exhibited by the well-recognised simplest ten-vertex bis(ligand) *arachno* species $B_{10}H_{12}L_2$ that are formed from two independent donor molecules [46], and it is also in contrast to the {*exo–endo*} configuration exhibited by compound **18** above (Fig. 11). It is structurally closely related to the similarly configured {*endo–endo*} non-metalla [μ-6,9-(PPh_2)-*arachno*-$B_{10}H_{12}$]$^-$ anion, which has been recognised for some time [49,50].

In view of these interesting reaction sequences exhibited by the ruthenium compounds **2a** and **2b**, and in view of the overall reduction summarised by Eq. (4) (see also Fig. 12), it is of interest to examine the corresponding reactions of the rhodium congener [6-(η^5-C_5Me_5)-*nido*-6-RhB_9H_{13}] (compound **16**) [51]. In our hands so far this has exhibited quite a different reactivity. Thus, from a more prolonged reaction of compound **16** with ethyl isocyanide, EtNC, the principal

isolated product is compound **22**, of formulation [1-(η^5-C_5Me_5)-*closo*-1,2-$RhCB_9H_9$-2-(NH_2Et)-7-(CNEt)] [Fig. 14 (upper)] [52]. In this species, a carbon atom of one of the ethyl isocyanide residues has been incorporated into the cluster – a phenomenon not observed in the ruthenium systems described above – and the resulting eleven-vertex cluster is of closed {$RhCB_9$} geometry. This *closo* configuration implies an overall cluster oxidation of the starting open-faced *nido*{RhB_9} cluster. Concomitant with this latter oxidation, there is a two-hydrogen reduction of the {EtN} residue of the cluster-assimilated EtNC unit to give an *exo*-cluster {NH_2Et} moiety, with an overall stoichiometry as in Eq. (6), in sum implying an additional dihydrogen loss from the system.

$$[(C_5Me_5)RhB_9H_{13}]\ \mathbf{16} + 2\mathrm{EtNC} \rightarrow [(C_5Me_5)RuCB_9H_9(CNEt)(NH_2Et)]\ \mathbf{22} + H_2 \quad (6)$$

In this last product **22** [Fig. 14 (upper)] the C–C–N–C skeletal strings of the two starting EtNC substrates can readily be traced, but this is not the case in the corresponding reaction with MeNC, in which the isolatable product is [1-(η^5-C_5Me_5)-*closo*-1,2,3-$RhC_2B_8H_9$-2-Me] [compound **23**, Fig. 14 (lower)]. Again a *closo* eleven-vertex geometry results, but now the cluster constitution is {RuC_2B_8}, implying the incorporation of two isocyanide carbon atoms into the cluster, and, also, showing the loss of a cluster boron atom. The C–N–C skeletal string units from the MeNC substrate are not now identifiable, as one cluster carbon atom is isolated in the cluster as a single {CH(*exo*)} unit, and the other cluster carbon atom is bound to a terminal methyl group; isocyanide nitrogen atoms are clearly lost [52]. There are clearly intriguing mechanistic questions here, not only concerning the fate of the nitrogen atoms, but also in the contrasting behaviour between (a) this rhodium system, in which the isocyanide carbon atoms are incorporated into the cluster to form metallacarbaborane units (compare the iridium and platinum systems above, near Eq. (3)), and (b) the ruthenium system more immediately above (e.g. Eq. (4), see also Fig. 12 above), in which the isocyanide unit is initially bound to the cluster and then reduced and extruded as amine.

By modification of the conditions of the ruthenium reaction, we have been able to isolate two products in which the structures show cluster characteristics that can be regarded as being at a point of notional decision related to that postulated for the acetylene reactions mentioned above: whether (a) to assimilate elements of the isocyanide unit, expel dihydrogen, and produce a condensed metallacarbaborane system, or (b) to reduce and extrude the intact elements of the isocyanide unit as an amine.

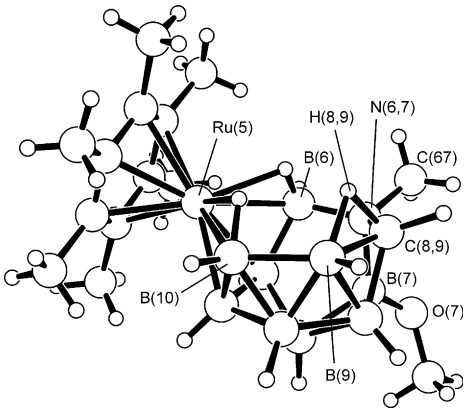

Fig. 15. Crystallographically determined molecular structure of the species **25** of formulation [(η^6-C_6Me_6)$RuCB_9N_{10}$(OMe)NMe] [52]. For a schematic line-drawings of the skeletal structure, see **V** and also Fig. 12. Selected interatomic distances (Å) are as follows: from Ru(5) to B(1) 2.221(1), to B(2) 2.252 (11), to B(6) 2.336(9), to B(10) 2.352(9) and to C(aryl) 2.183(6)–2.259(6); N(6,7) to B(6) is 1.488(10), to B(7) 1.528(12), to C(6,7) 1.484(10) and to C(8,9) 1.570(12); B(9)–H(8,9) is 1.50(1), C(8,9)–H(89) is 1.330(11) and B(7)–O(7) is 1.398(12).

Thus, firstly, reaction of MeNC with a substituent derivative of compound **2a**, specifically the B-methoxy-substituted *nido*-6-ruthenadecaborane [6-(η^6-C_6Me_6)-*nido*-6-RuB_9H_{12}-8-(OMe)] (compound **24**), gives the species **25**, of formulation [(η^6-C_6Me_6)$RuCB_9H_{10}$(OMe)NMe] [52]. Compound **25** (Fig. 15 and schematic cluster structure **V**) has an open {$RuCNB_9$} twelve-vertex cluster structure that has three open faces (bold lines in **V**). These three open faces consist of a six-membered RuBNCBB face, a five-membered BNBBB face, and a four-membered BNCB face. There are three bridging hydrogen atoms associated with the six-membered open face. The structure can be regarded in terms of a ten-vertex {MB_9} *quasi-nido*-5-ruthenadecaborane geometry (schematic cluster structure **VI**) with a {–NMe–CH_2–} unit bridging across between the B(7)–B(8), B(6)–B(7) and B(8)–B(9) {MB_9} cluster vectors, thereby engendering some ten-vertex *arachno* character in the {RuB_9} unit. The {–CH_2–} unit appears to exhibit a rare incidence of a carbon–hydrogen–boron open-face bridging hydrogen atom, and also indicates an incipient more complete accommodation of the isocyanide carbon unit into the cluster. There are relationships to the proposed intermediate **19** of formulation {(C_6Me_6)-$RuB_9H_{11}(CH_2NMe)$} discussed above (Fig. 12), which appears to have a more straightforward {–CH_2–} methylene unit [50,51]. In gross terms, a transfer of the open-face {Ru–H–B} bridging hydrogen atoms of compound **25** to the {CH_2NMe} moiety, with the extrusion of the latter as Me_2NH and cluster closure to [(C_6Me_6)-RuB_9H_8(OMe)], could be envisaged as a model for the final stages of the mechanistic pathway of Eq. (4) and Fig. 12.

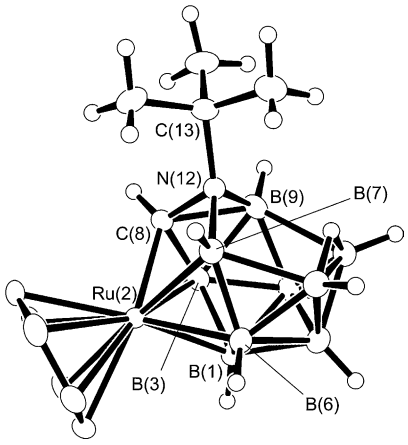

Fig. 16. Crystallographically determined molecular structure of [(η^6-C_6Me_6)$RuCB_9H_{10}N^{tert}Bu$] **26** (CCDC 255857). For schematic line-drawings of the skeletal structure, see **VIIA** and also Fig. 12. Selected interatomic distances (Å) are as follows: Ru(2) to B(1) 2.174(3), to B(3) 2.198(4), to B(6) 2.208(3), to B(7) 2.270(3), to C(8) 2.066(3) and to C(aryl) 2.244(3)–2.305(3); from N(12) to B(7) 1.608(4), to C(8) 1.478(4), to B(9) 1.561(4) and to C(13) 1.532(3); B(7)–B(11) is 1.990(5), B(9)–B(10) is 2.079(5) and B(10)–B(11) is 1.786(5).

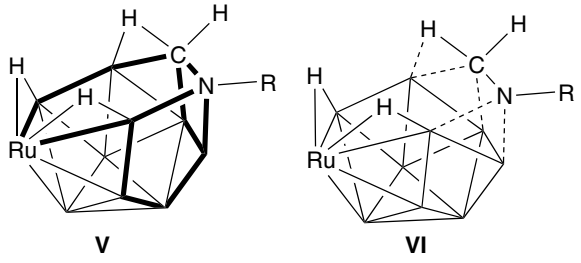

The second model for an intermediate, compound **26**, of formulation [(η^6-C_6Me_6)$RuCB_9H_{10}N^{tert}Bu$] (Fig. 16 and schematic cluster structure **VIIA**), is isolatable from the reaction between compound **2a** and ^{tert}BuNC. The cluster is seen to be more condensed than that of **25**, with only two open faces: four-membered {RuCNB} and five-membered {BNBBB} (bold lines in structure **VIIA**). There is now only one bridging hydrogen atom, which is associated with the {NB_4} five-membered open face. The isocyanide carbon atom is now more intimately associated with the structure than as in compound **25**, and, in general terms, a mechanism can be envisaged in which dihydrogen loss would convert a structure with the general shape of that of compound **25** (schematic **V**) to one with a shape like that of compound **26** (schematic **VIIA**). As with compound **25** (schematic **VI**), in compound **26** an *arachno*-type {MB_9} unit is again readily traced when the elements of the isocyanide string are removed from the cluster structure (hatched lines in schematic **VIIB**).

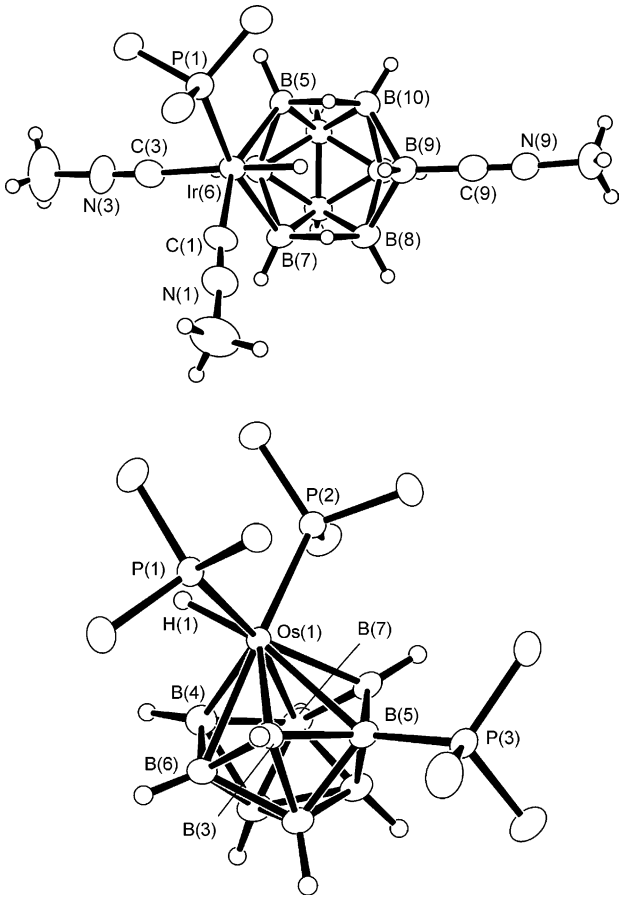

Fig. 17. Crystallographically determined molecular structures of (upper) the species [6,6,6,6-$(MeNC)_2(PPh_3)$H-*arachno*-6-IrB_9H_{11}-9-(CNMe)] **27** (CCDC 255858) and (lower) [1,1,1-$(PMe_2Ph)_2$H-*isocloso*-1-OsB_9H_8-5-(PMe_2Ph)] **30** (CCDC 255859) [53]. Selected interatomic dimensions (Å) are as follows. For **27**: from Ir(6) to C(1) 1.971(7), to C(3) 2.016(8), to B(2) 2.244(7), to B(7) 2.287(8), to B(5) 2.299(7), to P(1) 2.323(2), and to H(6) 1.56 (9); B(8)–B(9) is 1.858(12), B(9)–B(10) is 1.878(11), B(9)–C(9) is 1.533(11) and C(9)–N(9) is 1.141(9). For **30**: from Os(1) to B(2) 2.177(4), to B(3) 2.162(4), to B(4) 2.104(4), to P(1) 2.3966(11), to P(2) 2.3821(11), to to B(5) 2.437(4), to B(6) 2.408(4), to B(7) 2.412(4) and to H(1) 1.599(34); P(3)–B(5) is 1.909(4).

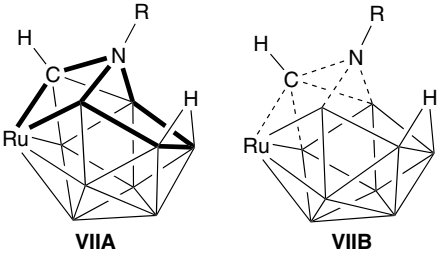

An extrusion of the {N^{tert}Bu} moiety from **26** could thence be visually entertained, to give the free amine $^{tert}BuNH_2$ and a closed cluster product, although from this particular species an additional redox process, for example by additional ^{tert}BuNC addition to give [(C_6Me_6)$RuCB_9H_9(CN^{tert}Bu)$], would be required for this to occur. In this regard, compound **26** models a pos-

sible structural type on the pathway to such species as **23** and **24** above, rather than being a direct analogue of an intermediate.

There will clearly be merit in the continued investigation of these and related metallaborane reaction systems, in order further to unravel details of these competing reaction processes and to see what other interesting structural types may emerge. There is also interest in the examination of the reactions of the isocyanides with the iridium species such as compound **5** and **8** mentioned above in view of the interesting reactions that these two iridaboranes undergo with acetylenes (e.g. Eqs. (1) and (2) above). However, the heating of [6,6,6-$(PPh_3)_2$H-*nido*-6-IrB_9H_{13}] (compound **8**) with MeNC at reflux in solution in CH_2Cl_2 gives only products related to the bis(alkylisocyanide) *arachno* compounds [Ar(RNC)MB_9H_{11}(CNR)] mentioned above (e.g. compound **18**, Fig. 11), rather than any species resulting either from incorporation of isocyanide carbon atoms into the cluster, or from reduction and extrusion of the MeCN unit. Thus the species [6,6,6,6-$(MeNC)_2(PPh_3)$H-*arachno*-6-IrB_9H_{11}-9-(CNMe) [compound **27**, Fig. 17 (upper)] is the predominant product [53]. Here, the *nido* compound **8** has therefore undergone a similar transformation to that undergone by [6-(η^6-$MeC_6H_4^{iso}$ Pr)-*nido*-6-RuB_9H_{13}] (compound **17b**) to give compound **18** (e.g. Eq. (5) above), but in addition has suffered a replacement of a PPh_3 ligand on the iridium centre by a methyl isocyanide ligand (Eq. (7)).

$$[(PPh_3)_2HIrB_9H_{13}]\ \mathbf{8} + 3MeNC \rightarrow [(MeNC)_2(PPh_3)HIrB_9H_{11}(CNMe)]\ \mathbf{27} + H_2 + PPh_3 \quad (7)$$

As with compound **18** (Fig. 11 above), the *arachno* configuration of the cluster unit of compound **27** [Fig. 17 (upper)] is readily apparent. The compound has open-face hydrogen atoms in the *endo* Ir(6) and B(9) positions, in a direct parallel to the very well-examined non-metal-containing decaboranyl analogues such as [6,9-$(MeCN)_2$-*ara- chno*-$B_{10}H_{12}$], which has methyl cyanide, rather than methyl isocyanide, ligands [54]. An interesting contrasting reaction, but yielding the same type of product, occurs in the reaction of compound **8** with MeCOOH, which yields [2,2-(CO)(PPh_3)-μ-2^O,9^O-$(MeCO_2)$-*closo*-2-IrB_9H_{11}-10-(PPh_3)] (compound **28**) of the same type of conventional *closo* ten-vertex [$L_3HIrB_9H_9L$] constitution as compound **7** (Fig. 5 above) [55].

In another interesting contrast, we have found that a phosphine osmium congener of compound **8**, viz. the species [6,6,6-$(PMe_2Ph)_3$-*nido*-6-OsB_9H_{13}] (compound **29**), reacts with ^{tert}BuNC to give a different type of product, now more related to the *isocloso* [$ArRuB_9H_9$] products **17a** and **17b** obtained as in Eq. (4) above. In this osmaborane reaction, the predominant metallaborane product is the species [1,1,1-$(PMe_2Ph)_2$H-*isocloso*-1-OsB_9H_8-5-(PMe_2Ph)] [compound **30**, Fig. 17 (lower)] [53]. However, we have not yet been able to investigate this reaction system for reduced and/or oligomerised isocyanide reaction products, although an interesting by-product is the five-vertex osmapentaborane [2,2,2-$(PMe_2Ph)_3$-*nido*-2-OsB_4H_8] (compound **31**) [53], a variant of the species [2,2,2-$(PPh_3)_2$(CO)-*nido*-2-OsB_4H_8], which has been known for some time [56].

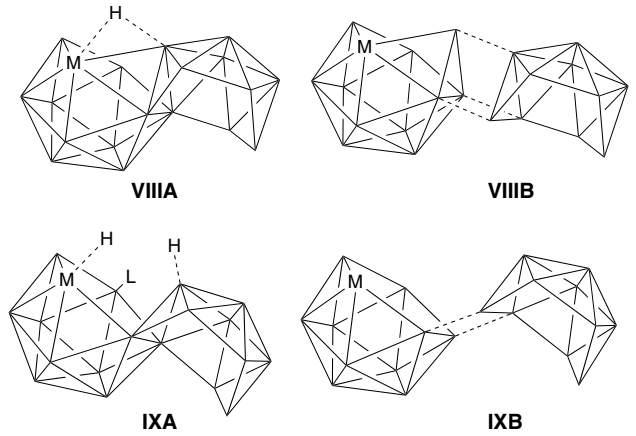

A further interesting variation in the reactions of isocyanides with metallaboranes is afforded by the reaction of MeNC with the macropolyhedral iridaborane **32** of

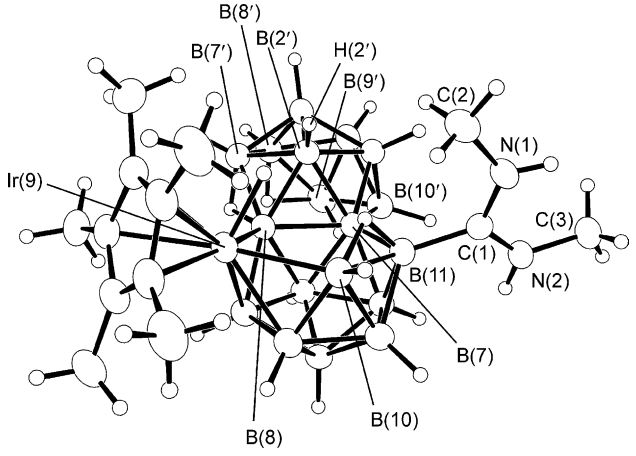

Fig. 18. Crystallographically determined molecular structure of [(η^5-C_5Me_5)$HIrB_{18}H_{19}${$C(NHMe)_2$}] **33** (schematic cluster structures **IXA** and **IXB**) [58] (CCDC 165856). Selected interatomic distances (Å) are Ir(9)–B(4) 2.170(4), Ir(9)–B(5) 2.178(5), Ir(9)–B(8) 2.203(4), Ir(9)–B(10) 2.234(4), Ir(9)–H(9) 1.6097, Ir(9)–C(C_5Me_5) 2.214(4)–2.254(4), B(7)–B(8) 1.890(5), B(7)–B(11) 1.885(5), B(7)–B(2′) 1.823(5), B(7)–B(10′) 2.038(6), B(8)–B(2′) 1.776(5), B(8)–B(7′) 1.871(6), B(10)–B(11) 1.917(6), B(7′)–B(8′) 1.934(6), B(8′)–B(9′) 1.797(7), and B(9′)–B(10′) 1.787(6), with other interboron distances between 1.726(6) and 1.823(6) Å for the {IrB_{10}} subcluster and between 1.706(6) and 1.809(6) Å for the {B_{10}} subcluster. Within the carbene ligand, B(11)–C(1) is 1.583(5), C(1)–N(1) is 1.326(4) and C(1)–N(2) is 1.311(5), with N(1)–C(2) 1.455(5) and N(2)–C(3) 1.445(5) Å, with angles B(11)C(1)N(1) 123.2(3), B(11)C(1)N(2) 118.5(3) and N(1)C(1)N(2) 118.3(3)°.

formulation $[(\eta^5\text{-}C_5Me_5)IrB_{18}H_{20}]$ (schematic configuration **VIIIA**). Compound **32** is a fused-cluster species, of the oligomerisations could be engendered by smaller, more accessible, boranes.

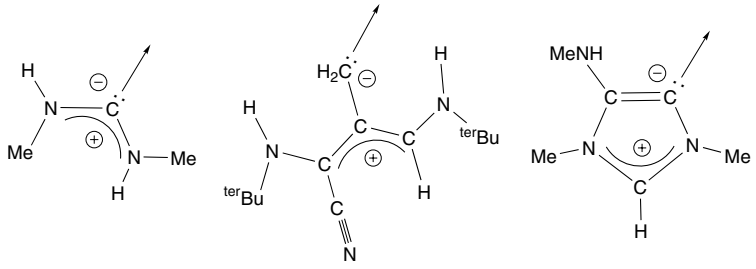

X **XI** **XII**

which the basic cluster structure consists of a *nido* twelve-vertex $\{IrB_{11}\}$ subcluster and a *nido* ten-vertex $\{B_{10}\}$ subcluster fused with three atoms in common (schematic **VIIIB**) [57,58]. The predominant product of the reaction of **32** with MeNC is $[(\eta^5\text{-}C_5Me_5)\text{-}HIrB_{18}H_{19}\{C(NHMe)_2\}]$ (compound **33**, Fig. 18, schematic cluster structure **IXA**) [58]. In compound **33**, the basic cluster structure now consists of an eleven-vertex *nido* $\{IrB_{10}\}$ subcluster and a *nido* ten-vertex $\{B_{10}\}$ subcluster, and now fused with only two boron atoms in common (schematic **IXB**). The essence of the reaction is the formal addition of the two-electron ligand $\{:CH(NHMe)_2\}$ to the cluster structure of compound **32** (schematically represented in Eq. (8)).

$$[(C_5Me_5)IrB_{18}H_{20}] + L \rightarrow [(C_5Me_5)HIrB_{18}H_{19}L] \qquad (8)$$

The carbene ligand $\{:C(NHMe)_2\}$ (schematic **X**) on the cluster of compound **31** merits brief further comment. There has been a reductive dimerisation of the MeNC units, but it is clear that the reaction has also involved the loss of one carbon atom. This type of process has also been recognised in reactions of ^{tert}BuNC and MeNC with the non-metal-containing macropolyhedral species *anti*-$B_{18}H_{22}$, from which products $B_{18}H_{20}L$ have been identified, where L is, for example, either of the two carbene ligands $\{(^{tert}BuNHCH)\{^{tert}BuNHC(CN)\}CH_2:\}$ (schematic **XI**) or $\{(MeNH)C_3N_2HMe_2\}$ (schematic **XII**) [59,60]. In the first of these two (schematic **XI**) a reductive oligomerisation of three ^{tert}BuNC units has occurred, with the loss, now, of two carbon atoms, together with an implied rearrangement; in the second (schematic **XII**) a reductive trimerisation has occurred, but now without carbon-atom loss, to give an imidazole-like ring. There may be scope here to tailor borane systems for the synthesis of polynitrogen organic species that may be difficult to obtain by other routes: for this to be practicable, however, a cleavage of the carbenes from the borane residue would have to be devised, and it would additionally be more practicable if

An additional feature worthy of comment is that the reaction of Eq. (8) represents one of the two competing consequences of the addition of electrons to a fused-cluster macropolyhedral species [61]: the addition of an electron-pair to a fused-cluster macropolyhedral species can either (a) open up one of the individual subclusters one step along the classical Williams–Wade *closo-nido-arachno*, etc. sequence, or (b) reduce the intimacy of inter-cluster fusion, here from a three-atoms-in-common to a two-atoms-in-common fusion mode. These competing principles are further illustrated by species such as $[(\eta^5\text{-}C_5Me_5)HIrB_{18}H_{19}(PMe_2Ph)]$ (compound **34**), which is isostructural in cluster terms with compound **33** (schematics **IXA** and **IXB** above). Such boron-ligated species can readily lose dihydrogen (Eq. (9)) to give species such as represented by $[(\eta^5\text{-}C_5Me_5)IrB_{18}H_{18}(PH_2Ph)]$ (compound **35**) [58,61]. The dihydrogen loss removes two electrons, one associated with each hydrogen atom, from the cluster bonding scheme. This results in an increase in the inter-cluster bonding intimacy from two-atoms-in-common, entailing a reversion to the three-atoms-in-common fusion mode (schematics **VIIIA** and **VIIIB** above).

$$[(C_5Me_5)HIrB_{18}H_{19}L] \rightarrow [(C_5Me_5)IrB_{18}H_{18}L] + H_2 \qquad (9)$$

These competing principles are further exemplified in the reaction of elemental sulphur with compound **33**. The product of this reaction, of anionic formulation $[(\eta^5\text{-}C_5Me_5)IrB_{18}H_{19}S]^-$ (species **36**) has a cluster architecture (schematic **XIIIA**) that consists of a *nido* twelve-vertex $\{IrB_{11}\}$ subcluster and an *arachno* ten-vertex $\{SB_9\}$ subcluster fused with two atoms in common (schematic **XIIIB**). Addition of the sulphur atom to the skeleton of compound **33** (schematic **VIIIA** above) has effectively added four extra electrons to the double-cluster system: two electrons reduce the fusion intimacy from three-atoms-in-common **VIII** to two-atoms-in-common **XIII**, and two electrons convert one of the two subclusters from *nido* to *arachno*.

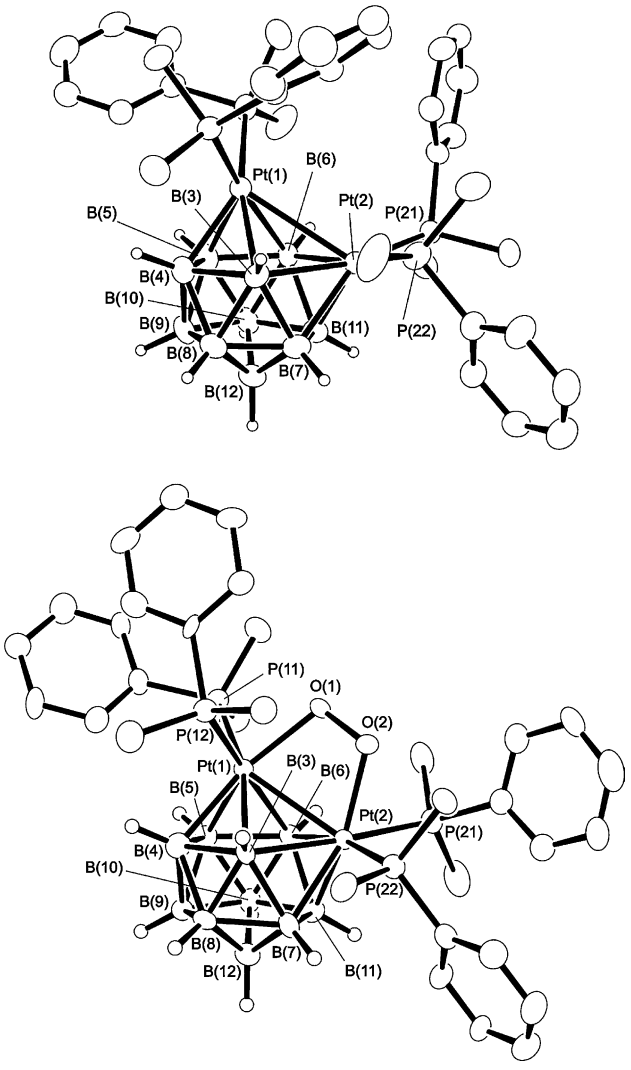

Fig. 19. Crystallographically determined molecular structures of (upper diagram) dark purple $[(PMe_2Ph)_4Pt_2B_{10}H_{10}]$ **37** (CCDC 115796) and (lower diagram) its dioxygen adduct $[(PMe_2Ph)_4(O_2)Pt_2B_{10}H_{10}]$ **39** (CCDC 235553) [67,68]. For **39**, there is crystallographically imposed twofold symmetry, so that Pt(1) = Pt(2), B(7) = B(4), B(8) = B(5), B(12) = B(10) and B(11) = B(9); selected interatomic distances (Å) for **37** are: from Pt(2) to Pt(1) 2.965(1), to P(1) 2.336(2), to P(2) 2.343(3), to B(6) 2.299(11), to B(7) 2.199(13) and to B(8) 2.238(12). The PPtP angle is 96.94(10)°, and the PtPtP angles are 114.84(6)° and 116.80(7)°. For **39**, selected interatomic distances (Å) are: from Pt(1) to Pt(2) 2.7143(3), to O(1) 2.141(4), to P(11) 2.3525(16), to B(3) 2.312(7), to B(4) 2.192(7), to B(5) 2.201(7), and to B(6) 2.291(7); from Pt(2) to O(2) 2.151(4), to P(21) 2.3898(16), to B(3) 2.287(7), to B(6) 2.317(7), to B(7) 2.212(7), and to B(11) 2.207(8); O(1)–O(2) is 1.434(6). There is a ca. 15° twist between the $\{O_2\}$ and the $\{Pt_2\}$ units, with torsion angles PtOOPt 19.9°, OPtPtO 10.6°, and OOPtPt 15.8° and 21.6°, and there are associated differences in the angles to phosphorus: Pt(2)Pt(1)P(11) and O(1)Pt(1)P(11) are 130.55(4)° and 86.38(12)°, respectively, whereas Pt(2)Pt(1)P(12) and O(1)Pt(1)P(12) are 117.08(4)° and 72.15(11)°, respectively. Pt(2)Pt(1)O(1) is 76.38(13)°, Pt(1)O(1)O(2) is 106.0(3)° and P(11)Pt(1)P(12) is 99.25(6)°: the corresponding angles around Pt(2) are similar to all these. In solution, the $\{O_2\}$ and the $\{(PMe_2Ph)_2\}$ units fluxionally exchange to their mirror positions either side of the Pt(1)Pt(2)B(9)B(12) plane, with $\Delta G^{\ddagger}$ (190–212 K) ca. 37.5 kJ mol^{-1} as measured by ^{31}P and ^{1}H NMR spectroscopy.

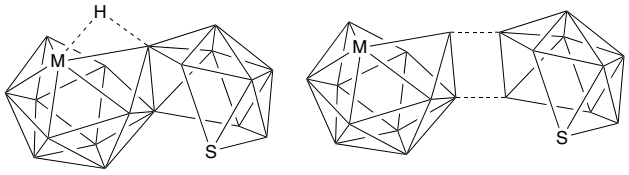

XIIIA **XIIIB**

Oxygen is in the same group as sulphur in the Periodic Table, and in view of sulphur addition to the macropolyhedral metallaborane **33** as mentioned in the last paragraph [57], and as also established for single-cluster metallaborane species [37,62], the reactivity of elemental oxygen with metallaboranes is of interest. Certainly the serendipitous incorporation of oxygen into metallaborane clusters has been noted, albeit rarely, for example in the oxaferraborane species $[(\eta^5\text{-}C_5H_5)FeOB_8H_{12}]$ [63], in oxarhodaborane species such as $[(\eta^5\text{-}C_5Me_5)RhOB_9H_{11}(NEt_3)]$ [64–66], and, most recently, in $[(\eta^6\text{-}C_6Me_6)RuOB_9H_{13}]$ [10]. We now have recently established an interesting dioxygen reaction with the dimetallaborane $[(PMe_2Ph)_4Pt_2B_{10}H_{10}]$ [compound **37**, Fig. 19 (upper)] [67]. Compound **37** is derived from *nido*-$B_{10}H_{14}$, not by the notional *replacement* of {BH(*exo*)} units by metal centres as in compounds **2a**, **2b** and **16** above, but by the experimentally realisable *addition* of two metal centres to the *nido*-decaboranyl cluster. It may be obtained, for example, by the successive addition of two $\{Pt(PMe_2Ph)_2\}$ units to the *nido*-decaboranyl residue by the utilisation of two successive treatments with $[PtCl_2(PMe_2Ph)_2]$ and non-nucleophilic base (Eqs. (10) and (11)) [28,67,68]. The intermediate species $[(PMe_2Ph)_2PtB_{10}H_{12}]$ (compound **38**) is well recognised [69–71].

$$B_{10}H_{14} + [PtCl_2(PMe_2Ph)_2] + 2\,\text{base} \rightarrow [(PMe_2Ph)_2PtB_{10}H_{12}]\ \mathbf{38} + 2\,\text{baseHCl} \quad (10)$$

$$[(PMe_2Ph)_2PtB_{10}H_{12}] + [PtCl_2(PMe_2Ph)_2] + 2\,\text{base} \rightarrow [(PMe_2Ph)_4Pt_2B_{10}H_{10}]\ \mathbf{37} + 2\,\text{baseHCl} \quad (11)$$

Compound **37** is a dark purple crystalline solid. It has a closed twelve-vertex $\{Pt_2B_{10}\}$ icosahedral cluster configuration, which is distorted from regular to accommodate the two platinum atoms, and in which the two platinum centres are adjacent, although not strongly connected, separation 2.965(1) Å. In solution, it rapidly takes up dioxygen across the {Pt–Pt} linkage to give a dark orange dioxygen adduct $[(PMe_2Ph)_4(O_2)Pt_2B_{10}H_{10}]$ [compound **39**, Fig. 19 (lower)]. In **39** the interplatinum distance has contracted to 2.7143(3) Å, and the overall cluster configuration is now that of a $\{Pt_2O_2\}$ *exo*-cluster four-membered ring fused to the twelve-vertex $\{Pt_2B_{10}\}$ icosahedron with the two platinum atoms held in common. The resulting *exo*-cluster Pt–O–O–Pt linkage is peroxidic in nature, and there has been consequently an effective oxidative addition of the dioxygen unit to

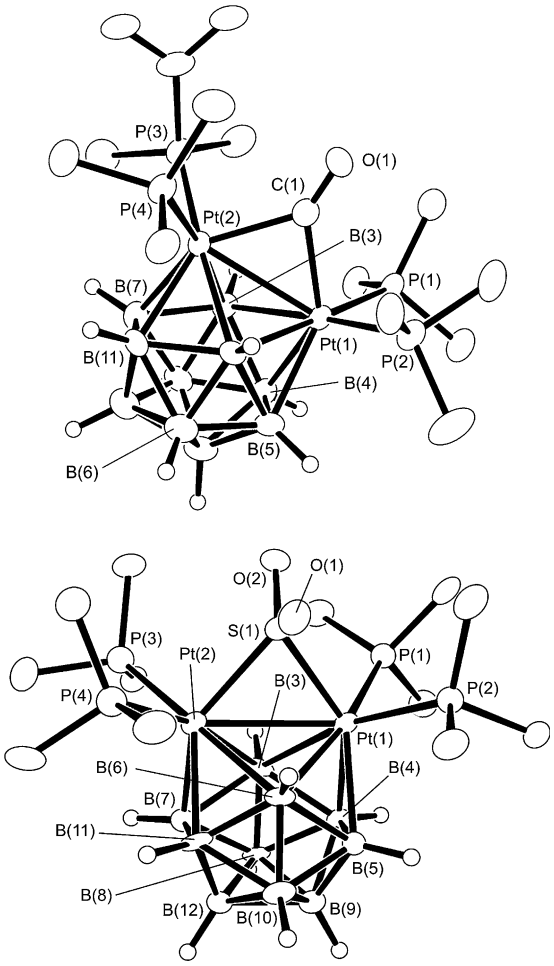

Fig. 20. Crystallographically determined molecular structures of adducts of compound **37**: (upper diagram) the CO adduct $[(PMe_2Ph)_4(CO)Pt_2B_{10}H_{10}]$ **40** (CCDC 254027) and (lower diagram) the SO_2 adduct $[(PMe_2Ph)_4(SO_2)Pt_2B_{10}H_{10}]$ **41** (CCDC 254028) [68]. Selected interatomic distances (Å) are as follows. For **40**: from Pt(1) to Pt(2) 2.7487(3), to C(1) 2.098(6), to P(1) 2.340(2), to P(2) 2.352(2), to B(3) 2.332(7), to B(4) 2.264(7), to B(5) 2.255(7) and to B(6) 2.305(6); from Pt(2) to C(1) 2.106(6), to P(3) 2.333(2), P(4) 2.344(2), to B(3) 2.298(7), to B(6) 2.348(7), to B(7) 2.271(7) and to B(11) 2.261(7); C(1)–O(1) is 1.174(7). For **41**: from Pt(1) to Pt(2) 2.8194(4), to S(1) 2.388(2), to P(1) 2.383(3), to P(2) 2.353(2), to B(3) 2.339(10), to B(4) 2.258(10), to B(5) 2.219(12), and to B(6) 2.322(10); from Pt(2) to S(1) 2.355(2), to P(3) 2.345(2), to P(4) 2.376(2), to B(3) 2.301(9), to B(6) 2.343(9), to B(7) 2.247(10) and to B(11) 2.261(11); S(1)–O(1) is 1.454(7) and S(1)–O(2) is 1.461(7).

the cluster. An interesting feature of the linkage is that it is fluxional: the $\{O_2\}$ unit is skewed relative to the Pt–Pt vector, across what would be a mirror plane in an idealised C_{2v} $\{Pt_2B_{10}\}$ unit, and the $\{O_2\}$ reversibly reverses its skew across this plane with a low activation energy of ca. 37.5 kJ mol^{-1}. An additional interesting feature is that the dioxygen uptake to give compound **39** is reversible. Gentle heating, reduction of pressure, or purging with an inert gas removes the dioxygen, and there is a consequent reversion to the dark purple compound **37** [67].

Such reversibility of dioxygen sequestration is reminiscent of the behaviour of the haems in mammalian blood, and in this regard the reaction of carbon monoxide with compound **37** is of interest. In this context we have found that the passage of carbon monoxide through a solution of **37** gives an immediate addition to form the yellow carbon monoxide adduct $[(PMe_2Ph)_4(CO)Pt_2B_{10}H_{10}]$ [compound **40**, Fig. 20 (upper)] [68]. In contrast to the dioxygen sequestration, this carbon monoxide addition is not reversible. Carbon monoxide also readily displaces dioxygen from **39** to give **40**, rather than adding to give a $\{CO_3\}$ carbonate bridge. The carbon atom of the {CO} unit in compound **40** bridges the two platinum atoms, and the oxygen atom projects radially out from the cluster. We have also found that sulphur dioxide similarly adds irreversibly across the $\{Pt_2\}$ unit, to give $[(PMe_2Ph)_4(SO_2)Pt_2B_{10}H_{10}]$ [compound **41**, Fig. 20 (lower)] [68]. In a similar manner to the carbonyl carbon atom in compound **40**, the sulphur atom bridges the two platinum atoms, with the two oxygen and the two platinum atoms generating an approximately tetrahedral disposition about the sulphur centre. As with the dioxygen adduct **39**, the interplatinum distances in compounds **40** and **41** are somewhat shorter than those in the starting compound **37**, at 2.7488(3) and 2.8194(4) Å, respectively.

3. Conclusions

In this survey of the reactions of a relatively small suite of metallaborane substrates with a relatively small selection of small reactive molecules, it is apparent that a rich variety of chemistry is revealed, presaged or suggested. All of the above reaction systems suggest future work, for example in terms of more detailed investigations of the individual systems to elucidate mechanisms for the processes, of which some are very unusual and therefore portend unpredicted chemistries, and also, for example, further work in the development of the new ideas and the new chemistries implicit in the results will also be valuable. In the small amount of work so far done, the emphasis of chemical elucidation has been on the metallaborane and metallaheteroborane products from these reactions; non-boron-containing products from the acetylene and isocyanide reactions in particular have not yet been investigated. It is hoped that this account will stimulate new work in these and related areas.

4. Experimental

The bulk of this overview article is based on reported species as given in individual references. The following summarises the experimental procedures and results for the reactions that gave the species in Figs. 2, 11, 16

and 17, for which such details are not reported elsewhere in the formal literature: $[NMe_4][(CO)_3WB_9H_9]$ **3a** [Fig. 2 (upper)], [6-(η^5-C_5Me_5)-6-(EtNC)-*arachno*-6-RhB_9H_{11}-9-(NCEt)] **18** [Fig. 11], [(η^6-C_6Me_6)$RuCB_9H_{10}N^{tert}Bu$] **26** Fig. 16], [6,6,6,6-$(MeNC)_2(PPh_3)$H-*arachno*-6-IrB_9H_{11}-9-(CNMe)] **27** [Fig. 17 (upper)] and [1,1,1-$(PMe_2Ph)_2$H-*isocloso*-1-OsB_9H_8-5-(PMe_2Ph)] **30** [Fig. 17 (lower)].

4.1. General

Initial reactions were carried out under a dry nitrogen atmosphere, with subsequent manipulations, chromatography, etc., carried out in air. Preparative thin-layer chromatography (TLC) was carried out using 1 mm layers of silica gel G (Merck, type GF254), made from water slurries on glass plates of dimensions 20 cm × 20 cm, followed by drying in air at 80 °C. Eluted TLC components were extracted from the silica matrix with CH_2Cl_2, and evaporated to dryness for further examination and or manipulation. HPLC was performed on a 16 mm × 25 cm column (Knauer, Lichosorb Si60, 7 mm), using a flow rate of 10 ml min^{-1}, with detection by change in the UV absorption of the eluant at λ = 254 nm. NMR spectroscopy was performed at ca. 2.3 and 9.4 T (fields corresponding to nominal 100 and 400 MHz ^{1}H frequencies, respectively) using commercially available instrumentation and using techniques and procedures as adequately described and enunciated elsewhere [72–78]. Spectra were recorded at 294–297 K for solutions in $CDCl_3$ or CD_3CN as indicated. Chemical shifts δ are given in ppm relative to Ξ = 100 MHz for $\delta(^1H)$ (±0.05 ppm) (nominally TMS), Ξ = 32.083972 MHz for $\delta(^{11}B)$ (±0.5 ppm) (nominally Et_2OBF_3 in $CDCl_3$) [72], and Ξ = 40.480730 MHz for $\delta(^{31}P)$ (±0.5 ppm) (nominally 85% aqueous H_3PO_4). Ξ is as defined by McFarlane [79]. Mass spectrometric data are from positive-ion 70 eV electron-ionisation spectra.

The minimum criterion of purity and identity consisted of the results of the single-crystal X-ray diffraction analysis experiments allied with clean multinuclear NMR spectra of the compounds in question.

4.2. Isolation of salts of the [1,1,1-(CO)$_3$-isocloso-1-$WB_9H_9]^{2-}$ anion 3

$[W(CO)_3(MeCN)_3]$ (100 mg, 250 μmol) and $[NMe_4]$[*nido*-B_9H_{12}] (90 mg, 500 μmol) were stirred in deoxygenated CH_2Cl_2 (25 ml) under N_2 for 3 h. The resulting brown precipitate was filtered off and washed with CH_2Cl_2 (3 × 10 ml) and then redissolved in MeCN (10 ml) to give a straw-coloured solution. Dropwise addition of Et_2O then resulted in a brown precipitate of the $[NMe_4]^+$ salt **3a** of the [1,1,1-$(CO)_3$-*isocloso*-1-$WB_9H_9]^{2-}$ anion **3** [Fig. 2 (upper)], which became somewhat lighter in colour upon drying in vacuo (12 mg, 20 μmol, 8%); ν_{max}(CO) 1890 and 1972 cm^{-1}. Cluster NMR data for **3a** (CD_3CN, 294 K): BH(2,3,4) +93.7 [+9.70], BH(8,9,10) +18.9 [+3.87], BH(5,6,7) −20.8 [−0.48], with $\delta(^1H)$ for $[NMe_4]^+$ at +3.09. Yields of between 4% and 5% of **3a** and of other salts of **3**, all of which were air-stable, were also similarly obtainable by performing the above procedure using the following salts of the [*arachno*-$B_9H_{14}]^-$ anion: $[NMe_4]$[*arachno*-B_9H_{14}] (90 mg, 480 μmol), $[NEt_4]$[*arachno*-B_9H_{14}] (120 mg, 500 μmol), and $[N^nBu_4]$[*arachno*-B_9H_{14}] (180 mg, 500 μmol). Purple crystals of the MeCN solvate of **3a**, suitable for the X-ray diffraction experiment summarised below, were grown by the overlayering with Et_2O of a concentrated solution of **3a** in MeCN in a 5 mm tube, and allowing slow diffusion to occur. The purple crystals lost MeCN over a few days at room temperature, yielding a tan powder.

4.3. Isolation of [6-(η^5-C_5Me_4)-6-(EtNC)-arachno-6-RhB_9H_{11}-9-(NCEt)] 18

[6-(η^5-C_5Me_5)-*nido*-6-RhB_9H_{13}] **16** (prepared as in [51]; 50 mg, 140 μmol) was dissolved in toluene (20 ml) and a solution of EtNC (15 mg, 280 μmol) in toluene (1.0 ml) was added, whereupon the colour of the solution changed from yellow to red. The reaction mixture was stirred for 45 min, the volatile components removed in vacuo, the residue dissolved in minimum CH_2Cl_2, and subjected to separation by preparative TLC using CH_2Cl_2 100% as liquid phase. The major component (yellow; R_F 0.8, 100% CH_2Cl_2) is characterised as [6-(η^5-C_5Me_4)-6-(EtNC)-*arachno*-6-RhB_9H_{11}-9-(NCEt)] **18** (Fig. 11) (43 mg, 90 μmol, 63%). Found for compound **18**: C 42.0, H 6.0, N 8.0%, calculated for $C_{16}H_{44}N_2B_9Rh$ C 42.1, H 6.1, N 8.0%; the mass spectrum (70 eV EI) exhibited a high-mass cut-off corresponding the highest-mass isotopomer of $C_{16}H_{36}N_2B_9Rh$. NMR data for **18** ($CDCl_3$, 294–297 K): BH(2) +16.5 [+3.50], BH(4) +8.5 [+3.25], BH(5,7) −2.0 [+2.24], BH(8,10) −18.1 [+1.96], BH(1,3) −31.7 [+0.84], BH(9) −37.8 [+0.55], with $\delta(^1H)$ for μH(5,7;8,10) at −3.13, for C_5Me_5 at +1.77 and for CH_2 at +3.77 and +3.63 (both 1:3:3:1 quartets, splitting ca. 7.3 Hz), and for CH_3 +1.47 (two accidentally coincident 1:2:1 triplets, splitting ca. 7.3 Hz). Crystals of **18** suitable for the X-ray diffraction experiment, summarised below, were grown by the overlayering with hexane of a concentrated solution of **18** in CH_2Cl_2 in a 5 mm tube, and allowing slow diffusion to occur.

4.4. Isolation of [(η^6-C_6Me_6)$RuCB_9H_{10}N^{tert}Bu$] 26

[6-(η^6-C_6Me_6)-*nido*-6-RuB_9H_{13}] **2a** (prepared as in [11]; 150 mg, 400 μmol) was dissolved in toluene (25 ml) and a solution of ^{tert}BuNC (70 mg, 800 μmol) in toluene (2.5 ml) was added. The reaction mixture was stirred for

20 min, the volatile components removed in vacuo, the residue dissolved in minimum CH_2Cl_2, and subjected to separation by preparative TLC using CH_2Cl_2 100% as liquid phase. The major yellow component (R_F 0.3; 100% CH_2Cl_2) is provisionally characterised by NMR spectroscopy as [6,6-(^{tert}BuNC)(η^6-C_6Me_6)-*arachno*-6-RuB_9H_{11}-9-($NC^{tert}Bu$)] **42** (94 mg, 175 μmol, 44%). There were several minor yellow components, of which one, of R_F ca. 0.95, after purification by repeated preparative TLC using CH_2Cl_2/hexane mixtures, is characterised as [(η^6-C_6Me_6)$RuCB_9H_{10}N^{tert}Bu$] **26** (Fig. 16) (R_F 0.75, CH_2Cl_2/hexane {50/50}; 8 mg, 20 μmol, 5%). We would hope to report on other products later. Found for compound **26**: C 44.6, H 8.5, N 3.4%, calculated for $C_{17}H_{37}NB_9$ Ru C 45.0, H 8.2, N 3.1%; the mass spectrum (70 eV EI) exhibited a high-mass cut-off corresponding the highest-mass isotopomer of $C_{17}H_{37}NB_9Ru$. NMR data for **26** ($CDCl_3$, 294–297 K), ordering {δ(^{11}B) [δ(^{1}H) of directly bound H(terminal) in square brackets]} +34.4 [+5.18], +33.0 [+5.52], +11.2 [+3.71], +10.4 [+1.62], +2.3 [+2.12], −7.5 [+2.10], −11.9 [+0.93], −12.9 [+1.54] and −27.2 [+0.91], with δ(^{1}H) for μH at −0.77, for C_6Me_6 at +2.21 and for ^{tert}Bu at +1.12; and for **42** ($CDCl_3$, 294–297 K) BH(2) +16.2 [+3.16], BH(4) +6.8 [+3.11], BH(5,7) −6.9 [+1.83], BH(8,10) −17.3 [+1.91], BH(1,3) −32.7 [+0.80] and BH(9) −40.5 [+0.59], with δ(^{1}H) for μH(5,7;8,10) at −3.35, for C_6Me_6 at +2.21 and for ^{tert}Bu at +1.49 and +1.43. Crystals of **26** suitable for the X-ray diffraction experiment, summarised below, were grown by the overlayering with hexane of a concentrated solution of **26** in CH_2Cl_2 in a 5 mm tube, and allowing slow diffusion to occur.

4.5. Isolation of [6,6,6,6-(MeNC)$_2$(PPh$_3$)H-arachno-6-IrB$_9$H$_{11}$-9-(CNMe)] 27

A solution of MeNC in CH_2Cl_2 (5.7 ml of a 0.074 M solution, corresponding to 422 μmol MeNC) was added to a solution of [6,6,6-$(PPh_3)_2$H-*nido*-6-IrB_9H_{13}] **8** (prepared as in [79]; 85 mg, 103 μmol) in CH_2Cl_2 (15 ml). The resulting solution was then heated to reflux temperatures and stirred at reflux for 4.5 h (during which time a colour change from bright yellow to very pale yellow was observed) and then cooled to room temperature. The volatile components were removed in vacuo, the residue dissolved in CH_2Cl_2 (ca. 5 ml) and subjected to separation by preparative TLC using CH_2Cl_2/hexane {60/40} as liquid phase, yielding three principal component bands, A at R_F ca. 0.45 (yellow), B at R_F ca. 0.25 (pale yellow) and C at R_F ca. 0.1 (two overlapping very pale yellow bands). Component mixture C was dissolved in CH_2Cl_2/hexane (90/10) (ca. 1.5 ml) and purified by HPLC, using CH_2Cl_2/hexane (90/10) as the liquid phase, to yield two colourless species, colourless [6,6,6,6-$(MeNC)_2(PPh_3)$H-*arachno*-6-IrB_9H_{11}-9-(CNMe)] **27** [Fig. 17 (upper)] (R_T 53-60 min; 28 mg, 31 μmol, 42%) and [6,6,6,6-$(MeNC)_2(PPh_3)$H-*arachno*-6-IrB_9H_{11}-9-(PPh_3)] **43**; (R_T 37-46 min; 24 mg, 26 μmol, 35%). Component A, upon crystallisation from CH_2Cl_2/hexane, yielded unreacted compound **8** (24 mg, 29 μmol, 28% recovery); ^{11}B NMR spectroscopy showed that component mixture B was a weak mixture of many boron-containing species. Colourless [6,6,6,6-$(MeNC)_2(PPh_3)$-H-*arachno*-6-IrB_9H_{11}-9-(CNMe)] **27** exhibited ν_{max}(NC) 2180 and 2200 cm^{-1}. Its mass spectrum (FAB ionisation) exhibited a high-mass cut-off at *m*/*z* 686 corresponding to the empirical formula $IrB_9C_{24}H_{35}N_3P$, i.e. the highest-mass isotopomer of the molecular ion (which would have *m*/*z* 687) minus one H atom. NMR data for **27** ($CDCl_3$, 297 K): BH(2) and BH(4) ca. +10 (accidentally coincident) [+4.32 and +4.00], BH(5) and BH(7) ca. −15 (accidentally coincident) [+2.50 and +2.27], BH(8) and BH(10) ca. −17 (accidentally coincident) [ca. +1.8 (accidentally coincident)], BH(1), BH(3) and BH(9) ca. −35 (all three accidentally coincident) [+1.03, +0.93 and +0.31], with δ(^{1}H) for μH(5,7) and μH(8,10) −3.58 and −4.72, for IrH −15.52 [doublet, ^2J(^{31}P–^{1}H) 16 Hz], and for MeNC +3.37 [singlet, bound to B(9)], +3.04 [bound to Ir(6), doublet, ^5J(^{31}P–^{1}H) ca. 1.5 Hz] and +2.96 [bound to Ir(6), doublet ^5J(^{31}P–^{1}H) ca. 1.6 Hz]; δ(^{31}P) ($CDCl_3$, 223 K) +9.1 ppm (sharp). Crystals suitable for the X-ray diffraction experiment, summarised below, were grown by slow evaporation from a concentrated solution of **27** in $CDCl_3$ held in a 5 mm tube. Colourless [6,6,6,6-$(MeNC)_2(PPh_3)$H-*arachno*-6-IrB_9H_{11}-9-(PPh_3)] **43** was tentatively characterised as such by comparison with **27**. It exhibited ν_{max}(NC) 2180 and 2200 cm^{-1}. Its mass spectrum (FAB ionisation) exhibited a high-mass cut-off at *m*/*z* 863 corresponding to the highest-mass isotopomer of the molecular ion (of which the empirical formula $IrB_9C_{40}H_{48}N_2P_2$ would give *m*/*z* 908) minus one MeNC unit and two dihydrogen units. NMR data for **43** ($CDCl_3$, 297 K): BH(2) and BH(4) ca. +9 (accidentally coincident) [+4.28 and +3.94], BH(5) and BH(7) ca. −14.5 (accidentally coincident) [+2.60 and +2.38], BH(8) and BH(10) ca. −18 (accidentally coincident) [ca. +1.79 and+1.70], BH(9) ca. −25.1 [+1.39], BH(1) and BH(3) (accidentally coincident) [+0.94 and +0.91], with δ(^{1}H) for μH(5,7) and μH(8,10) −3.22 and −4.40, for IrH −15.18 [doublet, ^2J(^{31}P–^{1}H) 16 Hz], and for MeNC +3.04 and +2.96 [both doublets, ^5J(^{31}P–^{1}H) ca. 1.5 Hz]; δ(^{31}P) ($CDCl_3$, 223 K) +16.1 (broader) and +8.9 ppm (sharper).

4.6. Isolation of [1,1,1-(PMe$_2$Ph)$_2$H-isocloso-1-OsB$_9$H$_8$-5-(PMe$_2$Ph)] 30 and [2,2,2-(PMe$_2$Ph)$_3$-nido-2-OsB$_4$H$_8$] 31

^{tert}BuNC (70 μl, 52 mg, 625 μmol) was added to a solution of [6,6,6-$(PMe_2\ Ph)_3$-*nido*-6-OsB_9H_{13}] **29** (prepared as in [80], 100 mg, 140 μmol) in toluene (15 ml),

which was then heated to reflux temperatures and stirred at reflux for 16 h (during which time a colour change from yellow to yellow–green was observed) and then cooled to room temperature. The volatile components were removed in vacuo, the residue dissolved in CH_2Cl_2 (ca. 5 ml) and subjected to separation by preparative TLC using CH_2Cl_2 100% as liquid phase, yielding three principal component bands, A at R_F ca. 0.85 (almost colourless), B at R_F ca. 0.5 (yellow) and C at R_F ca. 0.3 (yellow). The first of these, A, upon crystallisation from CH_2Cl_2/hexane, yielded [2,2,2-$(PMe_2Ph)_3$-*nido*-2-OsB_4H_8] **31** as a pale yellow solid (9 mg, 14 μmol, 10%), which darkened considerably over a few days, but with no apparent change in its NMR spectra; the mass spectrum (FAB ionisation) exhibited a high-mass cut-off at *m*/*z* 656 corresponding to the empirical formula $OsB_4C_{24}H_{41}P_3$, i.e. the highest-mass isotopomer of **31**. NMR data for **31** ($CDCl_3$, 293 K): BH(4) +3.2 [+6.05], BH(3,5) −11.9 [+2.61], BH(1) −38.3 [−0.29], with $\delta(^1H)$ for μH(3,4;4,5) at −2.14, for μH(2,3;2,5) at −11.69 [doublet structure $^2J(^{31}P–^1H)$ ca. 25 Hz], for PMe_2 at (B-coordinated PMe_2Ph ligand) at +1.74 [$^2J(^{31}P–^1H)$ ca. 13 Hz], for PMe_2(Os-coordinated PMe_2Ph ligands) +1.50 [$N(^{31}P–^1H)$ ca. 8 Hz] and +1.49 [$N(^{31}P–^1H)$ ca. 7.5 Hz]; in the ^{31}P spectrum ($CDCl_3$, 223 K)both expected resonance positions were accidentally coincident at $\delta(^{31}P)$ ca. −31 ppm. The second component, B, was further purified somewhat by TLC, using CH_2Cl_2/pentane {60/40} as liquid phase, yielding a yellow solid, R_F ca. 0.2, which was then re-dissolved in CH_2Cl_2/hexane {80/20} (ca. 2 ml) and purified by HPLC, using CH_2Cl_2/hexane {80/20} as the liquid phase, to yield a final bright yellow air-stable crystalline form of [1,1,1-$(PMe_2Ph)_2$H-*isocloso*-1-OsB_9H_8-5-(PMe_2Ph)] **30** [Fig. 17 (lower)] (R_T ca. 10.5 min; 15 mg, 21 μmol, 15%). The mass spectrum (FAB ionisation) exhibited a high-mass cut-off at *m*/*z* 709 corresponding to two Daltons fewer than the empirical formula $OsB_9C_{24}H_{42}P_3$, i.e. the highest-mass isotopomer of the molecular ion minus a dihydrogen molecule, perhaps signifying a P-methyl *ortho*-cycloboronation in the mass spectrometer. NMR data for **30** ($CDCl_3$, 294–297 K): BH(4) +81.8 [+9.91], BH(2,3) +75.3 [+9.26, doublet structure $^3J(^{31}P–^1H)$ ca. 16 Hz], BH(10) +19.0 [+4.59], BH(8,9) +13.9 [+4.01], BH(5) −23.1 [PMe_2Ph ligand site, no terminal H, observed splitting from $^1J(^{31}P–^{11}B)$ ca. 125 Hz], BH(6,7) −25.7 [−0.80], with $\delta(^1H)$ for OsH at −11.9 [1:2:1 triplet, $^2J(^{31}P–^1H)$ ca. 28 Hz], for PMe_2 (B-coordinated PMe_2Ph ligand) +1.58, for PMe_2 (Os-coordinated PMe_2Ph ligands) +1.50 and +1.40 [$N(^{31}P–^1H)$ ca. 12 Hz for both]; $\delta(^{31}P)$ ($CDCl_3$, 223 K) +36.3 (broader) and +14.7 pm (sharper). A sample for the X-ray diffraction analysis (see below) was obtained by slow diffusion of hexane, through a thin layer of benzene, into a concentrated solution of **30** in 1,2-$Cl_2C_2H_4$ in a 5 mm tube. The second component, C, was shown by ^{11}B NMR spectroscopy to be a complex mixture, of which no one component was present to any significant extent. The various TLC experiments also revealed several other minor yellow components, for which ^{11}B NMR spectroscopy similarly suggested other osmaboranes, which were, however, individually present in quantities too small for characterisation.

5. Single-crystal X-ray diffraction analysis

The previously unreported crystallographic data for compounds **1**, **2a**, **3**, **4**, **18**, **26**, **27** and **30** are summarised below. Data for compound **4** have been previously reported [17], but we have now been able to collect a better data set at low temperature. Solution and refinement programs were standard, and from the SHELX suite. Structural diagrams were prepared using the ORTEP-3 program [81].

For compound **1** (prepared as in [10]): [4-(η^6-C_6Me_6)-*nido*-4-RuB_5H_9] **1**, $C_{34.5}H_{57}B_{10}Cl_3OP_4Pt_2$, M = 1216.31, monoclinic, space group $P2_1/n$, a = 8.622(2), b = 10.175(2), c = 18.889(3) Å, β = 99.76(2)°, U = 1.632 nm^3, Z = 4, D_{calc} = 1.327 Mg m^{-3}, λ = 0.71069 Å (Mo K_α), μ = 8.38 mm^{-1}, T = ambient, R = 0.0318 for 2571 reflections with $I > 2.0\sigma(I)$, and R_w = 0.0322 for all 3049 unique reflections; CCDC 255652.

For compound **2a** (prepared as in [11]): [6-(η^6-C_6Me_6)-*nido*-6-RuB_9H_{13}] **2a**, $C_{12}H_{31}B_9Ru$, M = 373.73, monoclinic, space group $P2_1$ (no. 4), a = 843.3(2), b = 1345.8(3), c = 863.7(2) Å, β = 110.03(2)°, U = 0.9209 nm^3, Z = 2, D_{calc} = 1.347 Mg m^{-3}, λ = 0.71073 Å (Mo K_α), μ = 0.748 mm^{-1}, T = 290 K, R = 0.0266 for 1768 reflections with $I > 2.0\sigma(I)$, and R_w 0.0273 for 1828 observed reflections; CCDC 255653.

For the [1,1,1-$(CO)_3$-*isocloso*-1-$WB_9H_9]^{2-}$ anion **3** in its $[NMe_4]^+$ salt **3a** (prepared as described above): $[NMe_4]_2[(CO)_3WB_9H_9]$ **3a** (CH_3CN monosolvate), $C_{11}H_{33}B_9N_2O_3W(C_2H_3N)$, M = 563.60, orthorhombic, space group $P2_12_12_1$, a = 8.848(1), b = 15.636(3), c = 18.455(3) Å, U = 2.553 nm^3, Z = 4, D_{calc} = 1.466 Mg m^{-3}, λ = 0.71069 Å (Mo K_α), μ = 4.34 mm^{-1}, T = ambient, R = 0.0335 for 2308 reflections with $I > 2.0\sigma(I)$, and R_w = 0.0335 for 2507 unique reflections; CCDC 255654.

For compound **4** (prepared as in [17]): [1,1,1-$(PMe_3)_2$H-*isocloso*-1-IrB_8H_7-8-Cl] **4**, $C_6H_{25}B_8ClIrP_2$, M = 473.33, monoclinic, space group $P2_1/c$, a = 9.11600(10), b = 15.9100(2), c = 12.5990(2) Å, β = 99.738(1)°, U = 1800.97(4) $Å^3$, Z = 4, D_{calc} = 1.746 Mg m^{-3}, λ = 0.71073 Å (Mo K_α), μ = 7.175 mm^{-1}, T = 120(2) K, R_1 = 0.0638 for 3755 reflections with $I > 2.0\ \sigma(I)$, and wR_2 0.1682 for all 4131 independent reflections; CCDC 255860.

For compound **18** (prepared as described above): [6-(η^5-C_5Me_5)-6-(EtCN)-*arachno*-6-RhB_9H_{11}-9-(EtCN)] **18**, $C_{16}H_{36}B_9N_2Rh$, M = 456.67, triclinic, space group $P\bar{1}$,

$a = 8.9102(1)$, $b = 10.1790(1)$, $c = 13.3184(2)$ Å, $\alpha = 102.508(1)$, $\beta = 91.610(1)$, $\gamma = 91.479(1)°$, $U = 1178.17(2)$ Å^3, $Z = 2$, $D_{calc} = 1.287$ Mg m^{-3}, $\lambda = 0.71073$ Å (Mo K_α), $\mu = 0.729$ mm^{-1}, $T = 150(2)$ K, $R_1 = 0.0255$ for 4436 reflections with $I > 2.0\sigma(I)$, and wR_2 0.0666 for all 9102 independent reflections; CCDC 255856.

For compound **26** (prepared as described above): [(η^6-C_6Me_6)$RuCB_9H_{10}N^{tert}Bu$] **26**, $C_{22}H_{50}B_9N_2Ru$, $M = 541$, orthorhombic, space group $Pna2_1$ $a = 26.2710(5)$, $b = 8.5020(1)$, $c = 10.0930(1)$ Å, $U = 2254.33(6)$ Å^3, $Z = 4$, $D_{calc} = 1.594$ Mg m^{-3}, $\lambda = 0.71073$ Å (Mo K_α), $\mu = 0.714$ mm^{-1}, $T = 150(2)$ K, $R_1 = 0.0266$ for 4060 reflections with $I > 2.0\sigma(I)$, and wR_2 0.0669 for all 4289 independent reflections; CCDC 255857.

For compound **27** (prepared as described above): [6,6,6,6-$(MeNC)_2(PPh_3)$H-*arachno*-6-IrB_9H_{11}-9-(CNMe)] **27** ($CHCl_3$ bisolvate), $C_{24}H_{36}B_9IrN_3P(CHCl_3)_2$, $M = 925.82$, monoclinic, space group $P2_1/c$, $a = 10.0490(9)$, $b = 30.318(3)$, $c = 13.520(5)$ Å, $\beta = 95.650(5)°$, $U = 4017.8(6)$ Å^3, $Z = 4$, $D_{calc} = 1.530$ Mg m^{-3}, $\lambda = 0.71069$ Å (Mo K_α), $\mu = 3.785$ mm^{-1}, $T = 200(1)$ K, $R_1 = 0.0431$ for 5743 reflections with $I > 2.0\sigma(I)$, and wR_2 0.1160 for all 7060 independent reflections; CCDC 255858.

For compound **30** (prepared as described above): [1,1,1-$(PMe_2Ph)_2$H-*isocloso*-1-OsB_9H_8-5-(PMe_2Ph)] **30**, $C_{24}H_{42}B_9OsP_3$, $M = 710.97$, triclinic, space group $P\bar{1}$, $a = 9.757(2)$, $b = 10.204(2)$, $c = 16.593(2)$ Å, $\alpha = 87.721(12)°$, $\beta = 77.355(12)°$, $\gamma = 71.711(11)°$, $U = 1529.8(5)$ Å^3, $Z = 1$, $D_{calc} = 1.544$ Mg m^{-3}, $\lambda = 0.71069$ Å (Mo K_α), $\mu = 4.339$ mm^{-1}, $T = 200(1)$ K, $R_1 = 0.0197$ for 4818 reflections with $I > 2.0\sigma(I)$, and wR_2 0.0459 for all 5403 independent reflections; CCDC 255859.

6. Data for deposition

For convenience, it may be noted that crystallographic data for the previously crystallographically unreported species **1**, **2a**, **3**, **4**, **18**, **26**, **27** and **30** are deposited at the Cambridge Crystallographic Data Centre, CCDC, with deposition numbers **1** CCDC 255652; **2a** CCDC 255653; **3** (as its $[NMe_4]^+$ salt **3a**) CCDC 255654; **4** CCDC 255860; **18** CCDC 255856; **26** CCDC 255857; **27** CCDC 255858; and **30** CCDC 255859, as indicated in the text and figure captions for the individual compounds. Previous recent depositions associated with cited reports are for species **31**, **33**, **37**, **39**, **40** and **41**, with deposition numbers **31** CCDC 165856 [60]; **33** CCDC 165856 [58]; **37** CCDC 115796 [66] and CCDC 254127 [71]; **39** CCDC 235553 [66]; **40** CCDC 254027 [71]; and **41** CCDC 254028 [71]. These data can be obtained free of charge at www.ccdc.cam.ac.uk/conts/retrieving.html [or from the Cambridge Crystallographic Data Centre, 12 Union Road, Cambridge CB2 1EZ, UK; fax: (internat.) +44-1223/336-033; E-mail: deposit@ccdc.cam.ac.uk].

Acknowledgement

Much of the work has involved publicly funded support from the UK SERC and the UK EPSRC. Recent aspects of the work have been supported by personal financial contributions from JB, and some earlier aspects by personal financial contributions from Donna Kennedy, whom we thank. We also thank Simon Barrett and Xavier Fontaine for assistance with NMR spectroscopy. NNG is congratulated by his co-authors upon the attainment of his 80th birthday in very fine form.

References

[1] N.N. Greenwood, I.M. Ward, Chem. Soc. Rev. 3 (1974) 231.
[2] R.N. Grimes (Ed.), Metal Interactions with Boron Clusters, Plenum Press, New York, 1982.
[3] J.D. Kennedy, Prog. Inorg. Chem. 32 (1984) 519–679.
[4] J.D. Kennedy, Prog. Inorg. Chem. 34 (1986) 211–434.
[5] L. Barton, D.P. Srivastava, in: G. Wilkinson, F.G.A. Stone, E. Abel (Eds.), Comprehensive Organometallic Chemistry II, vol. 1, Pergamon Press, Oxford, UK, 1995, pp. 275–372 (Chapter 8).
[6] R.E. Williams, Inorg. Chem. 1 (1971) 210.
[7] K. Wade, J. Chem. Soc., Chem. Commun. (1971) 792.
[8] K. Wade, Adv. Inorg. Chem. Radiochem. 18 (1976) 1.
[9] R.E. Williams, Adv. Inorg. Chem. Radiochem. 18 (1976) 67.
[10] M. Bown, Organoruthenaborane chemistry, Thesis, University of Leeds, Leeds UK (1987); J. Bould, M. Bown, J.D. Kennedy, Collect. Czech. Chem. Commun. 2005, Submitted, paper no. 2005 0010.
[11] M. Bown, X.L.R. Fontaine, N.N. Greenwood, J.D. Kennedy, J. Organomet. Chem. 325 (1987) 233.
[12] M. Bown, X.L.R. Fontaine, N.N. Greenwood, J.D. Kennedy, M. Thornton-Pett, J. Organomet. Chem. 315 (1986) C1.
[13] J. Bould, J.D. Kennedy, M. Thornton-Pett, J. Chem. Soc., Dalton Trans. (1992) 563.
[14] B. Štíbr, J.D. Kennedy, E. Drdáková, M. Thornton-Pett, J. Chem. Soc., Dalton Trans. (1994) 229.
[15] J.D. Kennedy, Disobedient skeletons, in: J. Casanova (Ed.), The Borane–carborane–carbocation Continuum, Wiley, New York, 1998, pp. 85–116.
[16] I. Macpherson, Some new metallaborane chemistry of molybdenum and tungsten, Thesis, University of Leeds, Leeds, UK, 1987.
[17] J. Bould, J.E. Crook, N.N. Greenwood, J.D. Kennedy, W.S. McDonald, J. Chem. Soc., Chem. Commun. (1982) 346.
[18] See, for example, J.D. Kennedy, in: S. Heřmánek (Ed.), Boron Chemistry (IMEBORON VI), World Scientific, Singapore, 1987, pp. 207–243.
[19] X.L.R. Fontaine, N.N. Greenwood, J.D. Kennedy, I. Macpherson, M. Thornton-Pett, J. Chem. Soc., Chem. Commun. (1987) 476.
[20] J.D. Kennedy, in: W. Siebert (Ed.), Advances in Boron Chemistry, Royal Society of Chemistry, Cambridge, UK, 1997, pp. 451–462.
[21] J. Bould, D.L. Ormsby, H.-J. Yao, C.-H. Hu, J. Sun, R.-S. Jin, S.L. Shea, W. Clegg, T. Jelínek, N.P. Rath, M. Thornton-Pett, R. Greatrex, P.-J. Zheng, L. Barton, B. Štíbr, J.D. Kennedy, in: M. Davidson, A.K. Hughes, T.B. Marder, K. Wade (Eds.), Contemporary Boron Chemistry, Royal Society of Chemistry, Cambridge, UK, 2000, pp. 171–174.

[22] S.L. Shea, J. Bould, M.G.S. Londesborough, S.D. Perera, A. Franken, D.L. Ormsby, T. Jelínek, B. Štíbr, J. Holub, C.A. Kilner, M. Thornton-Pett, J.D. Kennedy, Pure Appl. Chem. 75 (2003) 1239.
[23] S.L. Shea, S.D. Perera, J. Bould, A. Franken, T. Jelínek, J.D. Kennedy, C.A. Kilner, M.G.S. Londesborough, M. Thornton-Pett, in: Yu. Bubnov (Ed.), Boron Chemistry at the Beginning of the 21st Century, Editorial URSS, Moscow, Russia, 2003, pp. 27–35.
[24] M.A. Beckett, J.E. Crook, N.N. Greenwood, J.D. Kennedy, J. Chem. Soc., Dalton Trans. (1986) 1879.
[25] M.A. Beckett, N.N. Greenwood, J.D. Kennedy, P.A. Salter, M. Thornton-Pett, J. Chem. Soc., Chem. Commun. (1986) 556.
[26] M.G.S. Londesborough, E.J. MacLean, S.J. Teat, M. Thornton-Pett, J.D. Kennedy, Chem. Commun. (2005) 1584.
[27] Part 2 of this series. R.S. Coldicott, J.D. Kennedy, M. Thornton-Pett, J. Chem. Soc., Dalton Trans. (1996) 3819.
[28] Part 7 of this series. Y.-H. Kim, Y.M. McInnes, P.A. Cooke, R. Greatrex, J.D. Kennedy, M. Thornton-Pett, Collect. Czech. Chem. Commun. 64 (1999) 938.
[29] See for example, and references therein: L.F. Tieze, U. Griesbach, O. Elsner, Synletters 7 (2002) 1109.
[30] See, for example, and references therein: B. Štíbr, Chem. Rev. 92 (1992) 225.
[31] J. Plešek, T. Jelínek, E. Drdáková, S. Heřmánek, B. Štíbr, Collect. Czech. Chem. Commun. 49 (1984) 1559.
[32] R.N. Grimes, in: G. Wilkinson, F.G.A. Stone, E. Abel (Eds.), Comprehensive Organometallic Chemistry I, vol. 1, Pergamon Press, Oxford, UK, 1982, pp. 459–542.
[33] R.N. Grimes, in: G. Wilkinson, F.G.A. Stone, E. Abel (Eds.), Comprehensive Organometallic Chemistry II, vol. 1, Pergamon Press, Oxford, UK, 1995, pp. 373–430.
[34] Part 1 of this series. J. Bould, P. Brint, J.D. Kennedy, M. Thornton-Pett, J. Chem. Soc., Dalton Trans. (1993) 2335.
[35] J. Bould, P. Brint, X.L.R. Fontaine, J.D. Kennedy, M. Thornton-Pett, J. Chem. Soc., Chem. Commun. (1989) 1763.
[36] J. Bould, W. Clegg, T.R. Spalding, J.D. Kennedy, Inorg. Chem. Commun. 2 (1999) 315.
[37] J. Bould, N.P. Rath, L. Barton, Organometallics 15 (1996) 4915.
[38] Part 10 of this series. J. Bould, M. Thornton-Pett, M.B. Hursthouse, S.J. Coles, J.D. Kennedy, Inorg. Chem. Commun. 8 (2005) 143.
[39] J.D. Kennedy, Main Group Met. Chem. 12 (1989) 149.
[40] J. Bould, P.A. Cooke, U. Dörfler, J.D. Kennedy, L. Barton, N.P. Rath, M. Thornton-Pett, Inorg. Chim. Acta 285 (1999) 290.
[41] J. Bould, N.P. Rath, L. Barton, J.D. Kennedy, Organometallics 17 (1998) 902.
[42] E.J. Ditzel, X.L.R. Fontaine, N.N. Greenwood, J.D. Kennedy, Zhu Sisan, M. Thornton-Pett, J. Chem. Soc., Chem. Commun. (1989) 1762.
[43] E.J. Ditzel, X.L.R. Fontaine, N.N. Greenwood, J.D. Kennedy, M. Thornton-Pett, J. Chem. Soc., Chem. Commun. (1989) 1262.
[44] E.J. Ditzel, X.L.R. Fontaine, N.N. Greenwood, J.D. Kennedy, M. Thornton-Pett, Z. Anorg. Allg. Chem. 616 (1992) 79.
[45] Y.-H. Kim, P.A Cooke, N.P. Rath, L. Barton, R. Greatrex, J.D. Kennedy, M. Thornton-Pett, Inorg. Chem. Commun. 1 (1998) 375.
[46] S.G. Shore, in: E.L. Muetterties (Ed.), Boron Hydride Chemistry, Academic Press, New York, 1973, pp. 79–174.
[47] X.L.R. Fontaine, J.D. Kennedy, J. Chem. Soc., Dalton Trans. (1987) 1573.
[48] J. Bould, U. Dörfler, M. Thornton-Pett, J.D. Kennedy, Inorg. Chem. Commun. 4 (2001) 544.
[49] M.A. Beckett, J.D. Kennedy, J. Chem. Soc., Chem. Commun. (1983) 575.
[50] M. Thornton-Pett, M.A. Beckett, J.D. Kennedy, J. Chem. Soc., Dalton Trans. (1986) 303.
[51] X.L.R. Fontaine, H. Fowkes, N.N. Greenwood, J.D. Kennedy, M. Thornton-Pett, J. Chem. Soc., Dalton Trans. (1986) 547.
[52] E.J. Ditzel, X.L.R. Fontaine, N.N. Greenwood, J.D. Kennedy, Zhu Sisan, B. Štíbr, M. Thornton-Pett, J. Chem. Soc., Chem. Commun. (1990) 1741.
[53] R.S. Coldicott, Reactions of Smaller Molecules with Metallaboranes and some Related Chemistry, Thesis, University of Leeds, UK, 1993.
[54] J.V.d.M. Reddy, W.N. Lipscomb, J. Chem. Phys. 31 (1959) 610.
[55] J. Bould, P. Brint, J.D. Kennedy, M. Thornton-Pett, L. Barton, N.P. Rath, Collect. Czech. Chem. Commun. 62 (1997) 1239.
[56] J. Bould, J.D. Kennedy, N.N. Greenwood, J. Organomet. Chem. 249 (1983) 11.
[57] S.L. Shea, T.D. McGrath, T. Jelínek, B. Štíbr, M. Thornton-Pett, J.D. Kennedy, Inorg. Chem. Commun. 1 (1998) 97.
[58] S.L. Shea, T. Jelínek, S.D. Perera, B. Štíbr, M. Thornton-Pett, J.D. Kennedy, Dalton Trans. (2004) 1521.
[59] T. Jelínek, J.D. Kennedy, B. Štíbr, M. Thornton-Pett, J. Chem. Soc., Chem. Commun. (1994) 1999.
[60] T. Jelínek, C.A. Kilner, S.A. Barratt, J.D. Kennedy, B. Štíbr, M. Thornton-Pett, Inorg. Chem. Commun. 8 (2005) in press, paper no. INOCHE 1814.
[61] S.L. Shea, T. Jelínek, S.D. Perera, B. Štíbr, M. Thornton-Pett, J.D. Kennedy, Inorg. Chim. Acta (Special Issue on Rhodium and Iridium Chemistry) 357 (2004) 3119.
[62] Part 4 of this series. Y.-H. Kim, R. Greatrex, J.D. Kennedy, Collect. Czech. Chem. Commun. 62 (1997) 1289.
[63] R.P. Micciche, J.J. Briguglio, L.G. Sneddon, Inorg. Chem. 23 (1984) 3992.
[64] E.J. Ditzel, X.L.R. Fontaine, H. Fowkes, N.N. Greenwood, J.D. Kennedy, P. MacKinnon, Zhu Sisan, M. Thornton-Pett, J. Chem. Soc., Chem. Commun. (1990) 1692.
[65] X.L.R. Fontaine, H. Fowkes, N.N. Greenwood, J.D. Kennedy, M. Thornton-Pett, J. Chem. Soc., Chem. Commun. (1985) 1722.
[66] B. Frange, J.D. Kennedy, Main Group Met. Chem. 19 (1996) 175.
[67] Part 9 of this series. J. Bould, Y.M. McInnes, M.J. Carr, J.D. Kennedy, Chem. Commun. (2004) 2380.
[68] Part 11 of this series. J. Bould, C.A. Kilner, J.D. Kennedy, Dalton Trans. (2005) in press, paper no. B419243E.
[69] S.K. Boocock, N.N. Greenwood, J.D. Kennedy, W.S. McDonald, J. Staves, J. Chem. Soc., Dalton Trans. (1981) 2573.
[70] J.D. Kennedy, B. Wrackmeyer, J. Magn. Reson. 38 (1980) 529.
[71] S.K. Boocock, N.N. Greenwood, J.D. Kennedy, J. Chem. Soc., Chem. Commun. (1980) 305.
[72] J.D. Kennedy, Boron, in: J. Mason (Ed.), Multinuclear NMR, Plenum Press, New York, USA, 1987, pp. 221–254 (Chapter 8 and references therein).
[73] See, for example, together with references therein: S. Heřmánek, Chem. Rev. 92 (1992) 325;
D. Reed, Chem. Soc. Rev. 22 (1993) 109.
[74] J.D. Kennedy, J. Staves, Z. Naturforsch., Teil B 34 (1979) 808.
[75] T.L. Venable, W.C. Hutton, R.N. Grimes, J. Am. Chem. Soc. 104 (1982) 4716, and 106 (1984) 29.
[76] X.L.R. Fontaine, J.D. Kennedy, J. Chem. Soc., Chem. Commun. (1986) 779;
J. Chem. Soc., Dalton Trans. (1987) 1573.
[77] See, for example, together with references therein: M.A. Beckett, M. Bown, X.L.R. Fontaine, N.N. Greenwood, J.D. Kennedy, M. Thornton-Pett, J. Chem. Soc., Dalton Trans. (1988) 1969;
G. Ferguson, J.D. Kennedy, X.L.R. Fontaine, Faridoon, T.R. Spalding, J. Chem. Soc., Dalton Trans. (1988) 2555.
[78] W. McFarlane, Proc. R. Soc. (London), Ser. A 306 (1968) 185.
[79] S.K. Boocock, J. Bould, N.N. Greenwood, J.D. Kennedy, W.S. McDonald, J. Chem. Soc., Dalton Trans. (1982) 713.
[80] M.A. Beckett, N.N. Greenwood, J.D. Kennedy, M. Thornton-Pett, J. Chem. Soc., Dalton Trans. (1986) 795.
[81] ORTEP-3, L.J. Farrugia, J. Appl. Crystallogr. 30 (1997) 565.